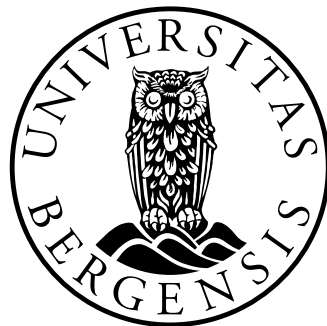


Performance of Distributed and Shared Memory Parallel Sparse Matrix Vector Multiplication

Kristian Sørdal



Thesis for Master of Science Degree at the University
of Bergen, Norway

2025

©Copyright Kristian Sørdal

The material in this publication is protected by copyright law.

Year: 2025

Title: Performance of Distributed and Shared Memory
Parallel Sparse Matrix Vector Multiplication

Author: Kristian Sørdal

Acknowledgements

To err is human; but to really foul things up requires a computer.

Paul R. Ehrlich

Abstract

SPARSE MATRIX VECTOR MULTIPLICATION is an important kernel used in scientific computing. It is a problem that lends itself well to parallelization. The problem is bounded by, and scales with the memory bandwidth of the system. Therefore in order to efficiently perform *SpMV* on large distributed memory systems, it is important to reduce the communication between nodes, in order to extract as much as possible out of the memory bandwidth of the system.

This thesis aims to investigate the results of *SpMV* when run using different communication strategies.

Contents

Acknowledgements	iii
Abstract	vii
1 Introduction	1
2 Theory	3
2.1 Sparse Matrix-Vector Multiplication	3
2.2 Definitions	4
2.3 Latency	4
2.4 Parallel Architectures	5
2.4.1 Shared Memory Architecture	5
2.4.2 Distributed Memory Architecture	5
2.4.3 Non-Uniform Memory Access	6
2.4.4 IPUs and emerging architectures	6
3 Background	7
3.1 CSR Storage Format	7
3.1.1 Computational Intensity	8
3.2 Other storage formats	8
3.2.1 COO Format	8
3.2.2 CSC Format	9
3.2.3 ELLPack Format	10
3.3 Sequential SpMV	10
3.4 Shared Memory SpMV	11
3.4.1 Scheduling options	12
3.4.2 Dynamic Scheduling	12
3.4.3 First-Touch Policy	13
3.4.4 Performance Implications of the First-Touch Policy	13
3.5 Distributed Memory SpMV	13
3.5.1 Load Balancing and Graph Partitioning	14

3.5.2	METIS	15
3.5.3	Hypergraph Partitioning	16
4	Communication Strategies	19
4.1	Strategy A - Exchange entire vector	20
4.2	Strategy B - Exchange only separators	21
4.2.1	Reordering	22
4.3	Strategy C - Exchange only required separators	24
4.4	Strategy D - Exchange only required separator values	26
4.5	Strategy E - Memory Scalable	27
5	Results	29
5.1	Theoretical Maximum	29
5.2	Matrices	29
5.3	Overview of Experiments	30
5.4	AMD EPYC 7601 - Single Node Performance	31
5.5	AMD EPYC 7601 - Multi Node Performance	42
5.5.1	2 proc per node	47
5.6	AMD EPYC 7302P - Multi Node Performance	51
5.7	AMD EPYC 7413 - Multi Node Performance	58
6	Related Work	65

Chapter 1

Introduction

Sparse Matrix Vector Multiplication (SpMV) is a fundamental computational kernel in numerous scientific and engineering applications, including numerical simulation, optimization, and machine learning. Due to its common presence in iterative solvers and graph based computations, improving the performance of SpMV remains a critical goal in the field of high performance computing. However, SpMV is inherently memory bound and characterized by irregular memory access patterns, which makes it challenging to achieve high computational efficiency.

Parallelization of SpMV offers a pathway to performance improvement, but the associated communication overhead becomes a primary bottleneck when operating in distributed memory environments. Unlike shared memory systems, where all processors can access a global memory space, distributed systems require explicit data exchanges between compute nodes. These communications often dominate the runtime cost, especially for large scale problems where data dependencies span across multiple nodes. The situation is exacerbated by the low computational intensity of SpMV operations, which further limits the benefits of increased computational resources unless communication is carefully managed.

This thesis aims to investigate the impact of different communication strategies on the performance of parallel SpMV in hybrid shared-distributed memory settings. By combining a shared memory model within individual compute nodes through the use of OpenMP and a distributed memory model for inter node communication using MPI, the study explores how various strategies, ranging from full vector broadcasts to minimal selective updates, affect both communication volume and execution time.

We evaluate several communication schemes, including:

- Full vector exchange, where the entire input or result vector is communicated across nodes.
- Separator based methods, where only the boundary elements (separators) are exchanged. Either through means of communicating the separator to all ranks, communicating it to only those ranks that require it through data-dependencies.
- Minimally selective communication, which restricts communication to only those separator values that are actually required for computation on neighbouring nodes.

These strategies are benchmarked on modern multicore architectures to assess their scalability and efficiency. Particular attention is paid to how different partitioning techniques, such as graph and hypergraph partitioning, influence the communication patterns and associated costs.

The central research question guiding this work is:

How do different communication strategies affect the performance of distributed SpMV, and what trade offs exist between communication volume, computational load balancing, and total execution time?

Chapter 2

Theory

2.1 Sparse Matrix-Vector Multiplication

Sparse Matrix-Vector Multiplication (SpMV) is a fundamental operation encountered in many areas of scientific computing. It is especially prominent in solving large systems of linear equations and in large-scale simulations. The matrices involved are typically both very large and very sparse.

A matrix can in theory be considered sparse if it is worthwhile to treat zero values separately. In theory, this translates to a matrix being less than full, i.e. less than $\mathcal{O}(n^2)$ nonzeros for a $n \times n$ matrix. However, in the context of sparse linear algebra, sparse means that there is a constant number of nonzeros per row, i.e. $\mathcal{O}(n)$ nonzeros per row. The matrices used in scientific computing, such as matrices based on meshes, or graphs such as social networks all have this property. Optimizing the performance of SpMV, particularly through parallel computing techniques, is crucial for enhancing the efficiency of many scientific applications.

However, SpMV is notoriously difficult to optimize, both in sequential and parallel implementations. One major reason is its inherently low computational intensity.

2.2 Definitions

Term	Definition
Node	A node, or a compute node, is a computeunit within a larger parallel computing system.
Dual/single socket	A dual or single socket node refers to the amount of processors on a node. Dual socketed nodes have two processors, that are connected through an interconnect.

2.3 Latency

The execution time of computational operations can vary significantly, and it is important to have some understanding of the latency times associated with typical operations. Referencing these latency numbers can be valuable when interpreting benchmark results and the performance of different programs.

Operation	Time [ns]
L1 cache reference	1
Branch misprediction	3
L2 cache reference	4
Mutex lock/unlock	17
Main memory reference	100
Compress 1K bytes with Zippy	2000
Send 2kB over 10 Gbps network	1600
Send 1K bytes over 1 Gbps network	10 000
Read 4K bytes randomly from SSD*	20 000
Round trip within same datacenter	500 000
Read 1MB sequentially from memory	1 000 000
Disk seek	10 000 000
Read 1MB sequentially from disk	10 000 000
TCP packet round trip between continents	150 000 000

Figure 2.1: Latency numbers for common operation, adapted from [9]

2.4 Parallel Architectures

There are two main architectures used in the parallel computing industry: Shared Memory Architecture and Distributed Memory Architecture. The following sections gives an overview of the key difference between the two.

2.4.1 Shared Memory Architecture

On a system with shared memory architecture, every processing unit (PU) have access to the same memory, treat it as a global address space. On such systems, the biggest challenge is that of *cache coherency*, where in order to prevent race conditions, every read of the cache must reflect the latest write (adapted from [7]).

2.4.2 Distributed Memory Architecture

On systems with distributed memory architecture, every processor have their own local memory, not accessible by other processors. When a process needs to access memory from another process, explicit communication of the data stored at that memory address needs to occur, and happens through whichever network the processors are connected with (adapted from [7]). Figure 2.2 shows the difference between shared and distributed memory architectures.

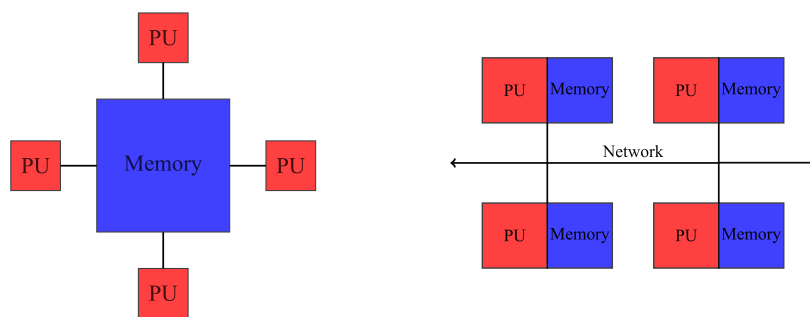


Figure 2.2: Shared and Distributed Memory Architecture (adapted from [6])

2.4.3 Non-Uniform Memory Access

Non-Uniform Memory Access (NUMA) refers to a multiprocessor system architecture in which memory access latencies depend on the location of the memory relative to a given processor. Unlike traditional symmetric multiprocessing (SMP) systems, where all processors share equal access times to a centralized memory pool, NUMA architectures consist of multiple processor sockets or nodes, each directly connected to its own local memory. These nodes are interconnected by a high-speed communication network, typically an interconnect, facilitating access to remote memory residing on other nodes.

2.4.4 IPUs and emerging architectures

In the ever evolving world of computer chip manufacturing, there has in the past years emerged a new trend in the field of architecture design. This comes in the form of packaging thousands of small processor cores into a single device, where each core has its own local memory, and no device-level shared memory [1]. An example of such a processor is the relatively new Cerebras Wafer-Scale Engine (WSE-3), which is the largest chip ever built. With a spec sheet of 4 trillion transistors, 900 000 cores, memory bandwidth of 21PB/s, and 44 GB of on-wafer memory (see [4]). Such architectures necessitates a careful distribution of relevant data across each processor, and is where memory scalable communication strategies are beneficial.

Chapter 3

Background

3.1 CSR Storage Format

CSR (Compressed Sparse Row) is the most widely used storage format for sparse matrices. As its name suggests, it compresses the amount of memory used to store a matrix without loss of information. It does so by utilizing three vectors A_p, A_j, A_x . Figure 3.1 shows an example of a matrix stored in CSR format, adapted from [3].

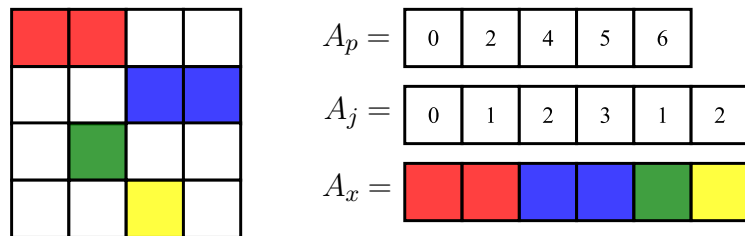


Figure 3.1: Matrix represented in the CSR format.

The first vector, A_p stores the indices of the first non-zero in the vectors A_p and A_x . For a given entry $A_p[i]$, $A_p[i]$ is the index of the first non-zero in the i^{th} row. $A_j[j]$ and $A_x[j]$ denotes the column index and value of the j^{th} non-zero, respectively.

Throughout the remainder of this thesis, we operate under the assumption that all matrices are represented in CSR format, unless explicitly noted otherwise.

3.1.1 Computational Intensity

The *computational intensity* of an operation describes the relation between the number of floating-point operations (FLOPS) and the number of memory accesses required. It is formally defined as:

$$\text{Computational intensity} = \frac{\text{FLOPS}}{\text{Memory accesses}} \quad (3.1)$$

Operations with low computational intensity, such as SpMV, are often *memory bound* rather than *compute bound*. This means that increasing the computational power of a system (e.g., faster processors) does not necessarily lead to proportional speedups in SpMV performance, as memory bandwidth remains the limiting factor.

3.2 Other storage formats

There exists many other lesser used storage formats for matrices

3.2.1 COO Format

The Coordinate List (COO) format stores the matrix as a set of triples on the form i, j, x , where i is the row index, j is the column index, and x is the value stored at (i, j) in the matrix. In this format all 0 entries are ignored.

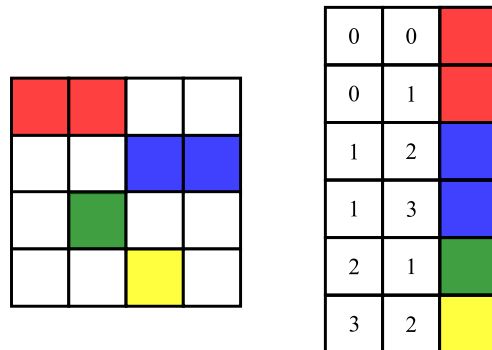


Figure 3.2: Example Matrix represented in the COO format.

3.2.2 CSC Format

The Compressed Sparse Column (CSC) format is similar to the CSR format, but instead of compressing the rows, we compress the columns. In this matrix format, we have irregular memory writes, but the reads are more regular. This can however be a problem

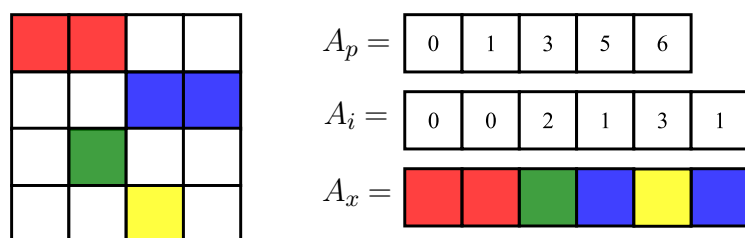


Figure 3.3: Matrix represented in the CSC format.

3.2.3 ELLPack Format

For an $M \times N$ matrix with a maximum of K non-zeros per row, the ELLPack format stores the non-zeros in an $M \times K$ matrix `data`, and an $M \times K$ matrix `indices`. The `data` matrix store the values of the non-zeros, and `indices` store the column index of every element. Rows that have fewer than K non-zeros are padded with zeros. Adapted from [12].

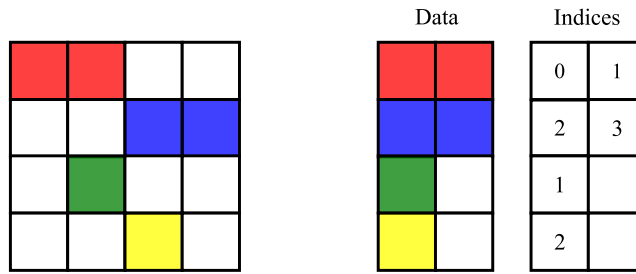


Figure 3.4: Matrix Represented in the ELLPACK format.

3.3 Sequential SpMV

A sequential implementation of SpMV on a matrix stored in the CSR format can be implemented in the following manner:

Algorithm 1: Sequential CSR-based SpMV

Input : A_p, A_j, A_x, x

Output : y

```

for  $i \leftarrow 0$  to  $n$  do
    sum  $\leftarrow 0$ 
    for  $j \leftarrow A_p[i]$  to  $A_p[i+1]$  do
        sum = sum +  $A_x[j] \cdot x[A_j[j]]$ 
     $y[i] \leftarrow$  sum

```

For SpMV on well structured matrices such as those similar to the matrix illustrated in Figure 3.5, each non-zero element typically incurs a data movement cost of approximately 12 bytes and results in 2 floating-point operations (FLOPs). This estimation may appear inconsistent with the data access pattern described in algorithm 3.3, where two double-precision values and one integer are accessed per non-zero, corresponding to a total of 20 bytes. The apparent discrepancy arises from the caching behavior of the input vector x : after the initial access, elements of x are frequently reused and thus remain in cache, reducing the effective memory traffic associated with subsequent accesses.

In contrast, for highly unstructured matrices, the absence of data locality can significantly degrade cache reuse. In the worst case scenario, each non-zero may trigger the loading of an entire 64 byte cache line, with only a small fraction of it being used. Consequently, the effective data movement can increase to as much as 76 bytes per 2 FLOPs.

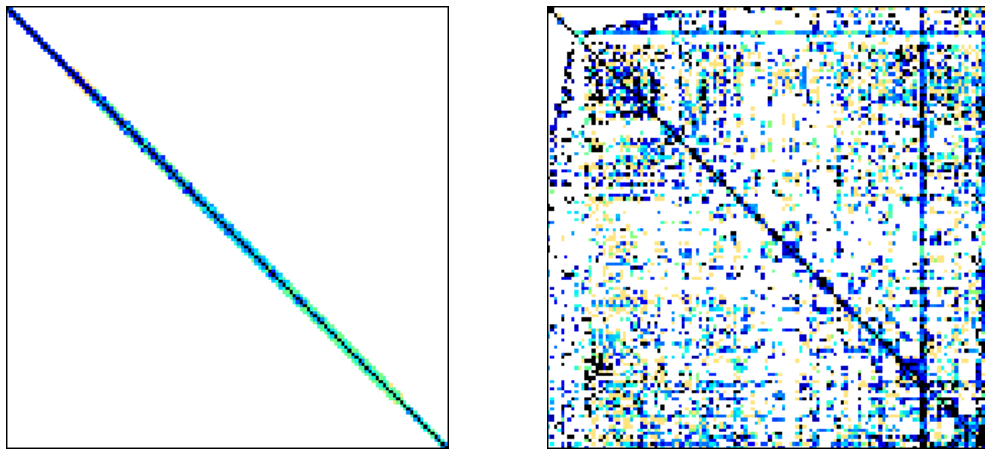


Figure 3.5: Well structured (a) and poorly structured (b) matrices.

3.4 Shared Memory SpMV

SpMV can be parallelized using the OpenMP directive `#pragma omp parallel for`. By default, this tells OpenMP to use `static` scheduling when parallelizing the outer iteration loop. When static scheduling is used, the span of the iteration that each thread will execute is precomputed, and stays static, as the naming suggests. There are other scheduling options, such as `dynamic` and `guided`, which will be discussed in later sections.

An implementation of shared memory SpMV is outlined below.

Algorithm 2: Shared Memory CSR-based SpMV

Input : A_p, A_j, A_x, x

Output : y

```
#pragma omp parallel for
for i ← 0 to n do
    sum ← 0
    for j ← Ap[i] to Ap[i + 1] do
        sum = sum + Ax[j] · x[Aj[j]]
    y[i] ← sum
```

3.4.1 Scheduling options

As seen in algorithm 2, the outer loop is parallelized, which translates to dividing the rows of the matrix evenly among the threads. This work fine for well structured matrices, but for matrices with dense rows, such as the matrix shown in Figure 3.6, we obtain large imbalances in the computational load for each thread, which impacts performance.

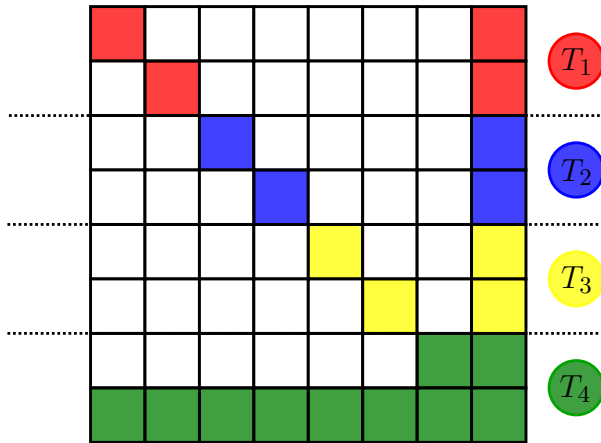


Figure 3.6: Row distribution among threads under static scheduling.

3.4.2 Dynamic Scheduling

Dynamic scheduling in OpenMP involves precomputing the range of iterations without assigning specific iteration subsets to individual threads

in advance. Under static scheduling, if thread A receives sparse rows and thread B receives dense rows, thread A will become idle prematurely while thread B remains computationally engaged. In contrast, dynamic scheduling allocates iterations at runtime to threads as they become available, thus potentially balancing the computational load more effectively, particularly when iteration workloads vary significantly.

At first glance, dynamic scheduling appears to resolve the workload imbalance inherent in static scheduling, even though it comes with more overhead. While this assumption holds true on smaller systems, such as personal laptops equipped with fewer physical cores and a single processor socket, it does not readily apply to larger, dual-socket systems utilized in this thesis. Here, the first-touch memory policy becomes particularly significant.

3.4.3 First-Touch Policy

The first-touch policy stipulates that the initial thread accessing a memory page allocates this page to its local memory domain. Consequently, if thread first accesses a memory page, it is stored locally to thread . Subsequent accesses by thread to this page result in non-local memory access, compelling thread to retrieve the data from either remote or main memory. Such accesses incur performance penalties due to significantly higher latency compared to local memory access.

3.4.4 Performance Implications of the First-Touch Policy

Table 2.1 illustrates that accesses to main memory exhibit substantially higher latency compared to local cache (e.g., L1 cache) accesses. In dual-socket configurations, accessing memory residing on the remote socket involves inter-socket communication through an interlink, further exacerbating latency. Consequently, dynamic (or guided) scheduling alone does not mitigate the performance degradation arising from poorly structured matrices, as it inadvertently exacerbates memory locality issues inherent to the first-touch policy on NUMA architectures.

3.5 Distributed Memory SpMV

In distributed memory systems, the computational workload is distributed across multiple nodes, each typically comprising a dual-socket architecture

with local memory. Unlike shared memory systems, data access across nodes is non-trivial and requires explicit communication, most commonly implemented using the Message Passing Interface (MPI).

For distributed sparse matrix-vector multiplication (SpMV), the computation proceeds similarly to the shared memory case (algorithm 2). The sparse matrix is divided across nodes, and each node computes its local segment of the output vector y . At the end of each iteration, partial results are assembled to produce the global vector, necessitating inter-node communication.

While the thread scheduling and memory locality issues discussed in 3.4.1 remain relevant, distributed memory systems introduce the additional challenge of communication overhead. As shown in Table 2.1, inter-node communication is significantly more expensive than memory accesses. Consequently, minimizing the total communication volume per SpMV iteration is critical for performance.

3.5.1 Load Balancing and Graph Partitioning

Even with a well-balanced distribution, excessive communication between nodes can become a performance bottleneck if data dependencies span many partitions. An effective partitioning strategy must therefore strike a careful balance between distributing the computational load evenly and reducing the amount of communication required between ranks. This trade-off is naturally captured by the graph partitioning problem.

The graph partitioning problem involves dividing an undirected graph $G(V, E)$, where V is the set of vertices and E is the set of edges into K disjoint subsets (or partitions) such that each subset contains a comparable amount of vertices, and the number of edges connecting different subsets is minimized. Each vertex $v_i \in V$ may be assigned a weight w_i , and each edge $e_{ij} \in E$ may carry a cost c_{ij} . The sum of weights W_k of each partition P_k must not exceed a specified imbalance threshold ϵ relative to the average weight of each partition. An edge can be classified as either an internal edge (those that connect nodes in the same partition), or an external edge (those that connect vertices in different partitions), and the cutsize is defined as the sum of the costs of all external edges. The goal is to minimize the cutsize, while preserving the balance between the size of each partition. This problem is known to be NP-Hard, even for obtaining bipartitions on unweighted graphs (adapted from [2]).

Algorithms that aim to solve the graph partitioning problem rely

on heuristics that provide good approximations in practice. Optimizing for one objective at the expense of the other is trivial but undesirable: assigning all vertices to a single partition minimizes communication to zero but results in extreme load imbalance, whereas naïvely assigning vertices to maintain balance without regard to connectivity may lead to high communication costs.

3.5.2 METIS

The graph partitioner used for the experiments in this thesis is called METIS. METIS is a software package for partitioning large irregular graphs, and has other uses such as partitioning meshes and computing fill-reducing orderings of sparse matrices. METIS provides algorithms that are based on multilevel graph partitioning. These algorithms partition the graph through a coarsening and refinement phase. In the coarsening phase, the size of the graph is reduced by way of collapsing the vertices and edges, and then partition the smaller graph. In the refinement phase, the graph is gradually expanded to its original size, and the portion of the graph that is close to the boundary is the primary focus, ensuring the quality of the partition is kept (adapted from [5]). algorithm 3 shows how to partition and reorder the vertices of a graph according to the generated partition, using METIS' K -way partition algorithm.

The way METIS partitions graph does not necessarily optimize for minimizing the communication volume, but rather obtaining partitions that are roughly equal in size. It is possible that there are partitions that have a larger imbalance between the size of partitions, but much smaller communication volumes. In order to obtain partitions that optimize for minimizing communication, it is necessary to look to hypergraph partitioners.

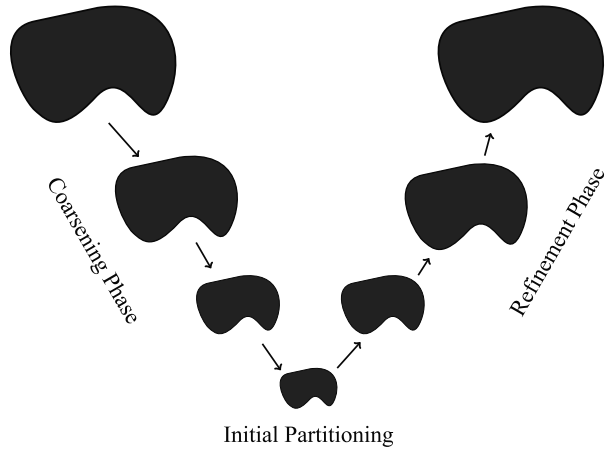


Figure 3.7: Illustration of multilevel graph partitioning (adapted from [5]).

3.5.3 Hypergraph Partitioning

A *hypergraph* $H = (V, N)$ is defined as a set of vertices V and a set of nets (hyperedges) N among those vertices. Every net $n_j \in N$ is a subset of vertices, i.e., $n_j \subseteq V$. The vertices in a net n_j are called its *pins* and denoted as $\text{pins}[n_j]$. The size of a net is equal to the number of its pins, i.e., $s_j = |\text{pins}[n_j]|$. The set of nets connected to a vertex v_i is denoted as $\text{nets}[v_i]$. The degree of a vertex is equal to the number of nets it is connected to, i.e., $d_i = |\text{nets}[v_i]|$.

[2]

Hypergraph partitioners try to solve the same problems, and employ similar algorithms as those graph partitioners use, however they use these algorithms on hypergraphs, and not regular graphs. Çatalyürek and Ayakanat showed in [2] that using the hypergraph partitioner they developed, they could get up to 63% less communication volume, with an average reduction in communication volume of 30% - 38%, when compared to METIS.

As the improvement of the communication strategies are the main focus of the contents of this thesis, the specific partitioner tool that is used is not the biggest concern, and the programs implemented have

opted for the usage of METIS, which as mentioned is a regular graph partitioner. It would be possible to refactor the code in such a way that a hypergraph partitioner such as PaToH can be used.

Algorithm 3: Partitioning and reordering a matrix.

Input : g, n_p, p

Output : Partitioned and reordered g

```

if  $n_p = 1$  then
     $p[0] \leftarrow 0$ 
     $p[1] \leftarrow g.n_r$ 
    return  $g$ 

partitionVector  $\leftarrow$  METIS_PartGraphKway(arguments
    specifying constraints for partition)
newId  $\leftarrow [0] \cdot g.n_r$ 
oldId  $\leftarrow [0] \cdot g.n_r$ 
id  $\leftarrow 0$ 
p[0]  $\leftarrow 0$ 
for  $r \in \{0, \dots, r\}$  do
    for  $i \in \{0, \dots, g.n_r\}$  do
        if  $partitionVector[i] = r$  then
            oldId[id]  $\leftarrow i$ 
            newId[i]  $\leftarrow id$ 
            id  $\leftarrow id + 1$ 
    partitionVector[r + 1]  $\leftarrow id$ 
newRowPtr  $\leftarrow [0] \cdot g.n_r + 1$ 
newColIdx  $\leftarrow [0] \cdot g.n_c$ 
newValues  $\leftarrow [0] \cdot g.n_c$ 
for  $i \in \{0, \dots, g.n_r - 1\}$  do
    d  $\leftarrow g.rowPtr[oldId[i] + 1] - g.rowPtr[oldId[i]]$ 
    newRowPtr[i + 1]  $\leftarrow newRowPtr[i] + d$ 
    for  $j \in \{0, \dots, d - 1\}$  do
        newColIdx[newRowPtr[i] + j]  $\leftarrow g.colIdx[g.rowPtr[oldId[i]]$ 
         $+ j]$ 
        newValues[newRowPtr[i] + j]  $\leftarrow g.values[g.rowPtr[oldId[i]]$ 
         $+ j]$ 
    for  $j \in \{newRowPtr[i], \dots, newRowPtr[i + 1] - 1\}$  do
        newColIdx[j]  $\leftarrow newId[newColIdx[j]]$ 
g.rowPtr  $\leftarrow newRowPtr$ 
g.colIdx  $\leftarrow newColIdx$ 
g.values  $\leftarrow newValues$ 
return g

```

Chapter 4

Communication Strategies

In parallel implementations of SpMV, effective communication management is critical due to its significant influence on overall performance. Communication often emerges as a bottleneck in distributed-memory systems because the speed at which data moves between nodes is significantly lower than within-node memory access speeds. Consequently, reducing communication volume and optimizing communication patterns can yield substantial performance improvements.

This chapter evaluates a series of progressively optimized communication strategies employed in distributed-memory parallel SpMV. Starting from the simplest method, exchanging the entire result vector between all nodes, the strategies become increasingly selective and efficient, focusing specifically on exchanging only the essential data elements required by each node. Finally, a communication strategy that is fully memory scalable is described. These approaches leverage knowledge of the matrix structure, partitioning methods, and computational dependencies to minimize communication overhead.

In the subsequent sections, each figure illustrating a communication strategy is based on the graph shown in Figure 4.1 as an example of a partitioned graph. In this example, each colour denotes the rank assigned to the vertices contained in the corresponding partition.

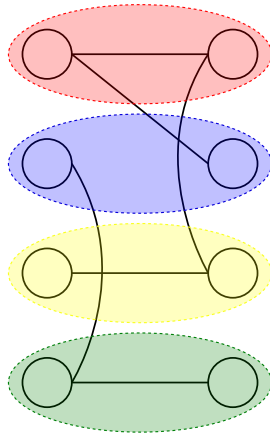


Figure 4.1: Simple graph partitioned amongst rank - each color represents a rank.

4.1 Strategy A - Exchange entire vector

In this strategy, at each iteration every rank sends its locally computed values of y to all other ranks so that each process obtains a complete copy of the output vector before proceeding. This approach can be implemented with the MPI collective operation `MPI_Allgatherv`, which supports different send and receive counts on each rank. 4 shows how this communication pattern can be implemented.

Algorithm 4: Strategy A - Communication Pattern

```

for each iteration do
    spmv(g,x,y)
    MPI_Allgatherv(local_y, sendcount, MPI_DOUBLE, y,
                  recvcounts, displs, MPI_DOUBLE, MPI_COMM_WORLD)
    swap pointers of x and y
  
```

Let n_p denote the total number of ranks, and let $|x_i|$ be the number of vector entries assigned to rank i (given by the average; $\frac{|x|}{n_p}$). Since each rank must send its local block size of $|x_i|$ to the other $n_p - 1$ ranks, the total volume of communication per iteration is given by 4.1.

$$\text{Total Communication} = n_p \cdot (n_p - 1) \cdot |x_i| \quad (4.1)$$

Figure 4.2 illustrates the state of the vector before and after communication using this strategy.

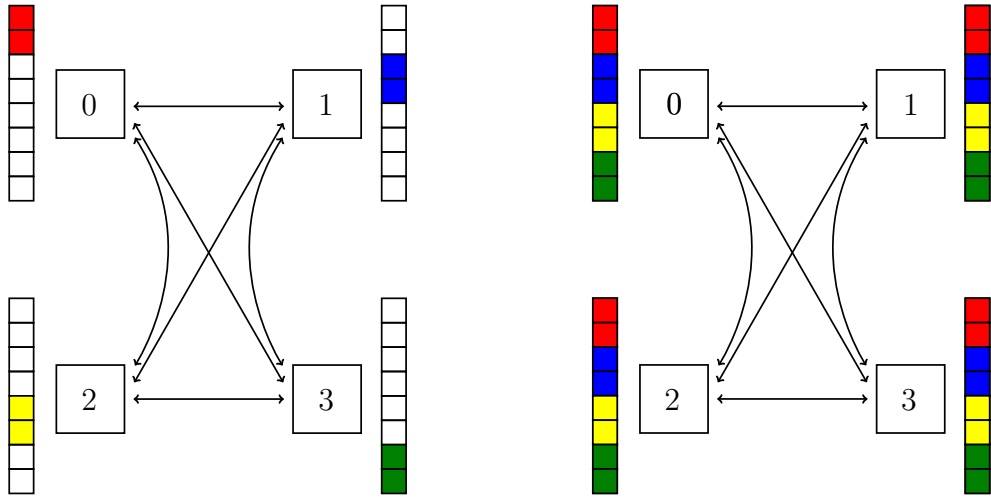


Figure 4.2: Contents of each rank's vector before and after communication under the *Exchange Entire Vector* communication pattern.

4.2 Strategy B - Exchange only separators

An improvement to the previous strategy can be achieved by recognizing that only separator values, those required by multiple processes, must be communicated. Non-separator values are used exclusively by the process that computed them and therefore do not need to be communicated.

Let n_p denote the total number of ranks, and let s_i be the size of the separator of rank i . Since each rank sends its separator to each other rank (i.e. $n_p - 1$ other ranks), then the total communication volume is given by 4.2.

$$\sum_{i=1}^{n_p} (n_p - 1) \cdot s_i \quad (4.2)$$

To facilitate this strategy, separator values are reordered such that they appear at the beginning of each process's local segment of y . Once this structure is established, communication is performed using `MPI_Allgatherv`, transmitting only the subset of y that contains separator values. The number of separators on each process must be known beforehand, which can be computed by counting the number of elements that have neighbours belonging to a different partition.

4.2.1 Reordering

After partitioning the matrix into different parts, we obtain a partition vector p , where the $p[i]$ stores the index of the partition the i^{th} entry in A_p . It is necessary to reorder the entries in A_p in accordance with the partition vector, such that all entries belonging to the same partition are stored in sequence. The algorithm below gives an outline of how this can be achieved. Here n_p is the number of partitions, n_r is the size of A_p , and n_c is the size of A_j and A_x .

Algorithm 5: Reordering of Separators

```

Input :  $n_p, n_r, n_c, p, A_p, A_j, A_x$ 
Output : Reordered  $A_p, A_j, A_x$ 

newId  $\leftarrow [0] \cdot n_r$ 
oldId  $\leftarrow [0] \cdot n_r$ 
id  $\leftarrow 0$ 
 $p_0 \leftarrow 0$ 

for  $r \in \{0, \dots, n_p - 1\}$  do
  for  $i \in \{0, \dots, n_r - 1\}$  do
    if  $p[i] = r$  then
      oldId[id]  $\leftarrow i$ 
      newId[i]  $\leftarrow id$ 
      id  $\leftarrow id + 1$ 
     $p[r + 1] \leftarrow id$ 

  newV  $\leftarrow [0] \cdot (n_r + 1)$ 
  newE  $\leftarrow [0] \cdot n_c$ 
  newA  $\leftarrow [0] \cdot n_c$ 

  for  $i \in \{0, \dots, n_r - 1\}$  do
    degree  $\leftarrow A_p[\text{oldId}[i] + 1] - A_p[\text{oldId}[i]]$ 
    newV[i + 1]  $\leftarrow newV[i] + degree$ 

  for  $i \in \{0, \dots, n_r - 1\}$  do
    degree  $\leftarrow A_p[\text{oldId}[i] + 1] - A_p[\text{oldId}[i]]$ 
    for  $j \in \{0, \dots, degree - 1\}$  do
      newE[newV[i] + j]  $\leftarrow A_j[A_p[\text{oldId}[i]] + j]$ 
      newA[newV[i] + j]  $\leftarrow A_x[A_p[\text{oldId}[i]] + j]$ 
    for  $j \in \{newV[i], \dots, newV[i + 1] - 1\}$  do
      newE[j]  $\leftarrow newId[newE[j]]$ 

```

Overwrite $A_p \leftarrow newV$, $A_j \leftarrow newE$, $A_x \leftarrow newA$

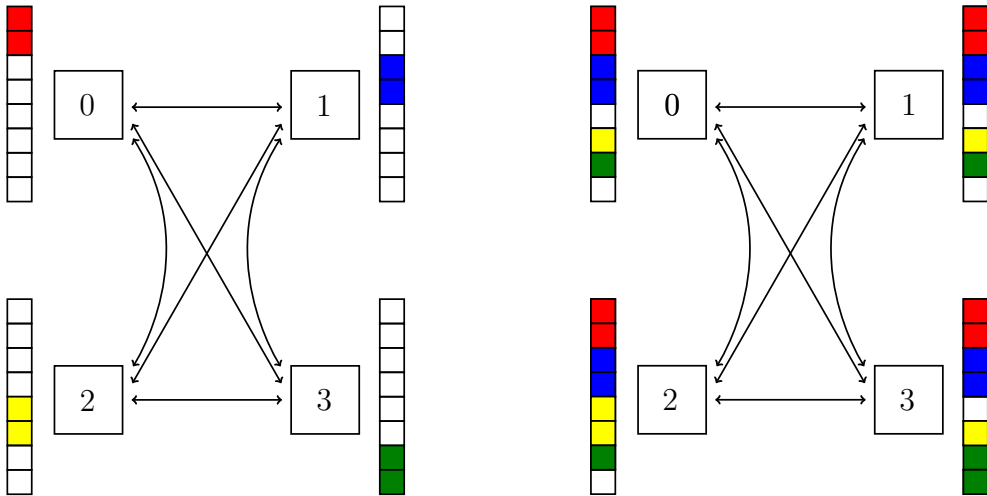


Figure 4.3: Contents of each ranks x vector before and after communication under the *Exchange Separators* communication pattern.

4.3 Strategy C - Exchange only required separators

Further reduction to the communication volume can be achieved by observing that not all separator values are required by every process. As the number of partitions increases, the set of dependencies between partitions tends towards sparsity. As a consequence of this, certain sets of separators may only need to be communicated to a given subset of processes. Using this strategy, each process only communicates its set of separator values to the processes that require them. The communication pattern is illustrated in Figure 4.4, and Algorithm 6 shows how this can be implemented.

Let n_p be the total number of ranks, n_i be the number of neighbours of rank i , and s_i the size of the separator of rank i . With $n_i \leq n_p$, the total communication volume is given by 4.3.

$$\sum_{i=1}^{n_p} s_i \cdot n_i \quad (4.3)$$

Algorithm 6: Exchange only required separators

Input : y , rank, size, displacements, sendItems, sendCount

Output :

```

MPI_Requests ← 0
for  $r = 0; r < size; r++$  do
    if  $rank = r$  or  $sendItems[r][rank] = 0$  then
         $\sqcup$  continue
        Post non-blocking MPI receive for  $sendCount[r]$  elements at
        address  $y + displacements[r]$ 
    MPI_Requests++
for  $r = 0; r < size; r++$  do
    if  $rank = r$  or  $sendItems[r][rank] = 0$  then
         $\sqcup$  continue
        Post non-blocking MPI send of  $sendCount[rank]$  elements to
        address  $y + displacements[rank]$ 
    MPI_Requests++
Wait for all non-blocking requests to complete

```

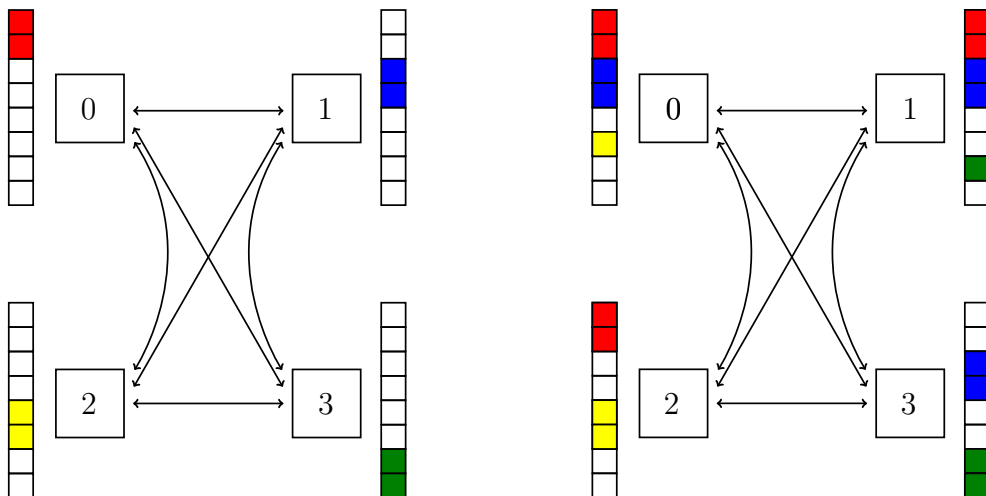


Figure 4.4: Contents of each ranks x vector before and after communication under the *Exchange Required Separators* communication pattern.

4.4 Strategy D - Exchange only required separator values

The final strategy further reduces the communication volume by only communicating the separator elements to the rank with which that element induces a data dependency. This approach eliminates all unnecessary data transfers but introduces additional complexity in managing communication schedules. It requires careful management of the send and receive lists, and introduces some additional overhead by means of a packing and unpacking step necessary for transmitting the data between ranks. This overhead does however not outweigh the benefits gained from the reduction in communication volume which this strategy yields.

Both strategy B and C requires reordering of the separator values, in order to make the communication of the separators easier, but due to the packing and unpacking step required for this strategy as seen in algorithm 7, reordering the separator elements is not required for this communication strategy.

Let n_p be the total number of ranks, and let d_i be the number of elements in rank i separator that are required by other ranks. Since this communication strategy only communicated these elements, the total communication volume is given by 4.4.

$$\sum_{i=1}^{n_p} d_i \quad (4.4)$$

Algorithm 7: Strategy D - Packing, exchanging and unpacking separator elements

```

Input :c, x, rank, size
Output :Updated vector x
totalSend, totalRecv ← 0
for  $i = 0; i < size; i++ \text{ do}$ 
   $\quad\quad\quad$  totalSend ← totalSend + c.sendCount[i]
   $\quad\quad\quad$  totalRecv ← totalRecv + c.receiveCount[i]
Allocate sendBuffer[totalSend], recvBuffer[totalRecv]
sendOffset ← 0
for  $i = 0; i < size; i++ \text{ do}$ 
   $\quad\quad\quad$  for  $j = 0; j < c.sendCount[i]; j++ \text{ do}$ 
     $\quad\quad\quad\quad\quad$  sendBuffer[sendOffset++] ← x[c.sendItems[i][j]]
Compute sendDispls, recvDispls as prefix sums of c.sendCount,
c.receiveCount
MPI_Ialltoallv(sendBuffer, c.sendCount, sendDispls, recvBuffer,
c.receiveCount, recvDispls)
MPI_Waitall()
recvOffset ← 0
for  $i = 0; i < size; i++ \text{ do}$ 
   $\quad\quad\quad$  for  $j = 0; j < c.receiveCount[i]; j++ \text{ do}$ 
     $\quad\quad\quad\quad\quad$  x[c.receiveItems[i][j]] ← recvBuffer[recvOffset++]
Free sendBuffer, recvBuffer, sendDispls, recvDispls
  
```

4.5 Strategy E - Memory Scalable

The communication strategies discussed so far all have a common problem that prevents them from scaling to large matrices. These strategies all store the entire vector x , and will run into performance issues when x is so large that it doesn't fit into memory. Usually, this is not a problem when SpMV is ran on CPUs, as they have large amounts of memory. Even on GPUs this problem might not be encountered, as modern GPUs have sufficient memory for large matrices.

Instead of storing the entire vector, each rank only stores its local part of the vector. In addition, it is necessary to allocate enough space for the separators elements that are needed from the other ranks. In order to achieve this, x is renumbered such that every ranks part of the vector is 0-indexed. For the local part of the x vector this is done by simply subtracting the position of the first local entry assigned to that rank from

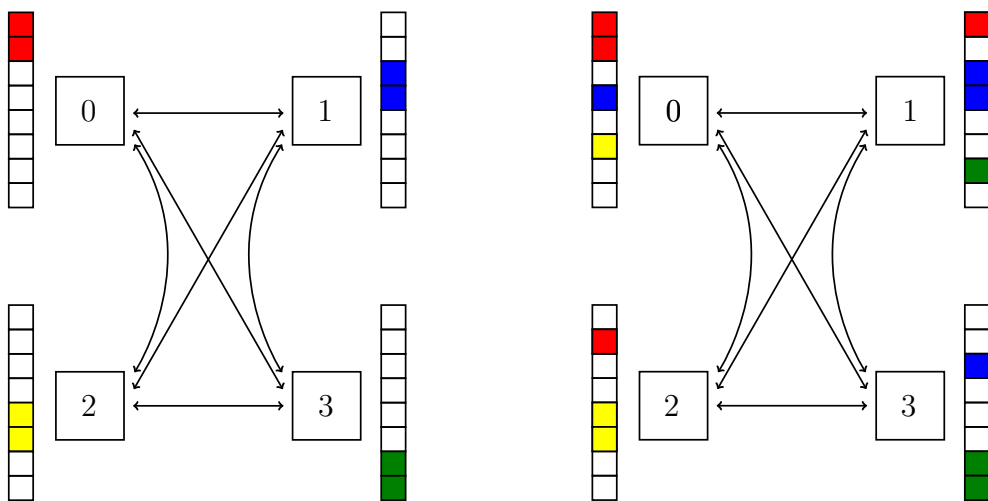


Figure 4.5: Contents of each ranks x vector before and after communication under the *Exchange Required Elements* communication pattern.

each entry in the local vector. It is also necessary to reorder the separator elements, as they will be stored after the entries in the local vector. This is achieved in a similar manner as the algorithm outlined in 5.

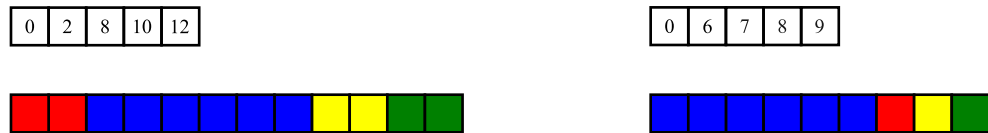


Figure 4.6: Global indexing vs. Local indexing of x .

Chapter 5

Results

5.1 Theoretical Maximum

As has been established, the maximum performance scales with the available memory bandwidth of the system, and not with the amount of processes used. For SpMV, a total of 6 bytes are read per FLOP, which means that the theoretical maximum is given by 5.1. This is under the assumption that all resources on the system is dedicated to the SpMV operation, which is not the case in reality. At most, somewhere in the neighbourhood of 80% of the systems resources can be expected to be utilized.

$$\text{Maximum Theoretical Performance} = \frac{\text{Memory bandwidth}}{6} \quad (5.1)$$

5.2 Matrices

As the field of interest is that of results from scientific computing, the matrices shown in Figre 5.1 have been selected. Matrices that are based on scientific computing problems are generally well structured and have nonzero entries centered around the main diagonal. Matrices with these kinds of structures tend to yield a larger cache hit rate than matrices based on social networks and other kinds of graphs. It is important to keep this in mind when interpreting the results, as other kinds of graphs can yield very different results.

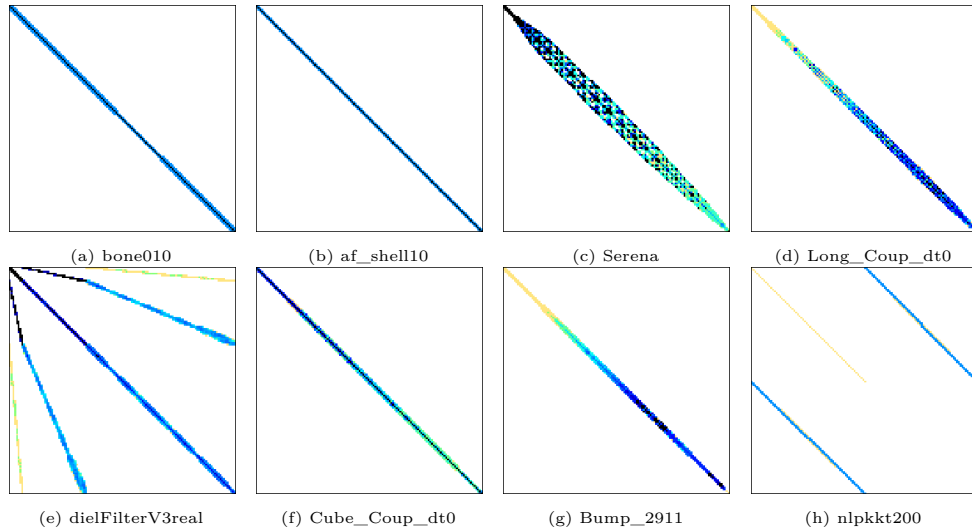


Figure 5.1: Matrices used to generate results.

Name	Purpose
bone010	Trabecular Bone Micro-Finite Element Model
af_shell1	Sheet metal forming matrix
Serena	Gas reservoir simulation for CO_2 sequestration
Long_Coup_dt0	3D coupled consolidation problem (geological formation)
dielFilterV3real	High-order vector finite element method in EM
Cube_Coup_dt0	3D coupled consolidation problem (3D cube)
Bump_2911	3D geomechanical reservoir simulation
nlpkkt200	Symmetric indefinite KKT matrix

5.3 Overview of Experiments

The experiments that have been ran in order to obtain the results in the following thesis have made use of systems on the Experimental Infrastructure for Exploration of Exascale Computing (eX³).

For each experiment, every matrix has been put through 100 iterations of SpMV, and every communication strategy has been tested on different configurations. For the single node experiments, each communication strategy has been ran with the number of MPI ranks being doubled until every available physical core on the chip is assigned one MPI rank. For multi node experiments on single socketed nodes, one MPI rank is assigned to each rank, and shared memory parallelization has been used

within each node. On dual socketed nodes, experiments placing one MPI rank per node and placing one MPI rank per socket have been ran. All programs have been compiled with `-march=native` and `-O3` compilation flags.

In the following presentation of the results, ?? gives an overview of what the different strategies will be referred to, both when analyzing the results, and in the legends of the figures.

Strategy name	Strategy Description
Strategy A	Exchanges entire local vector.
Strategy B	Exchanges entire separator.
Strategy C	Exchanges required separator.
Strategy D	Exchanges required separator elements
Strategy E	Exchanges required separator elements, memory scalable

5.4 AMD EPYC 7601 - Single Node Performance

The results in this section illustrates the performance of the communication strategies when performed on a single node containing two AMD EPYC 7601 chips.

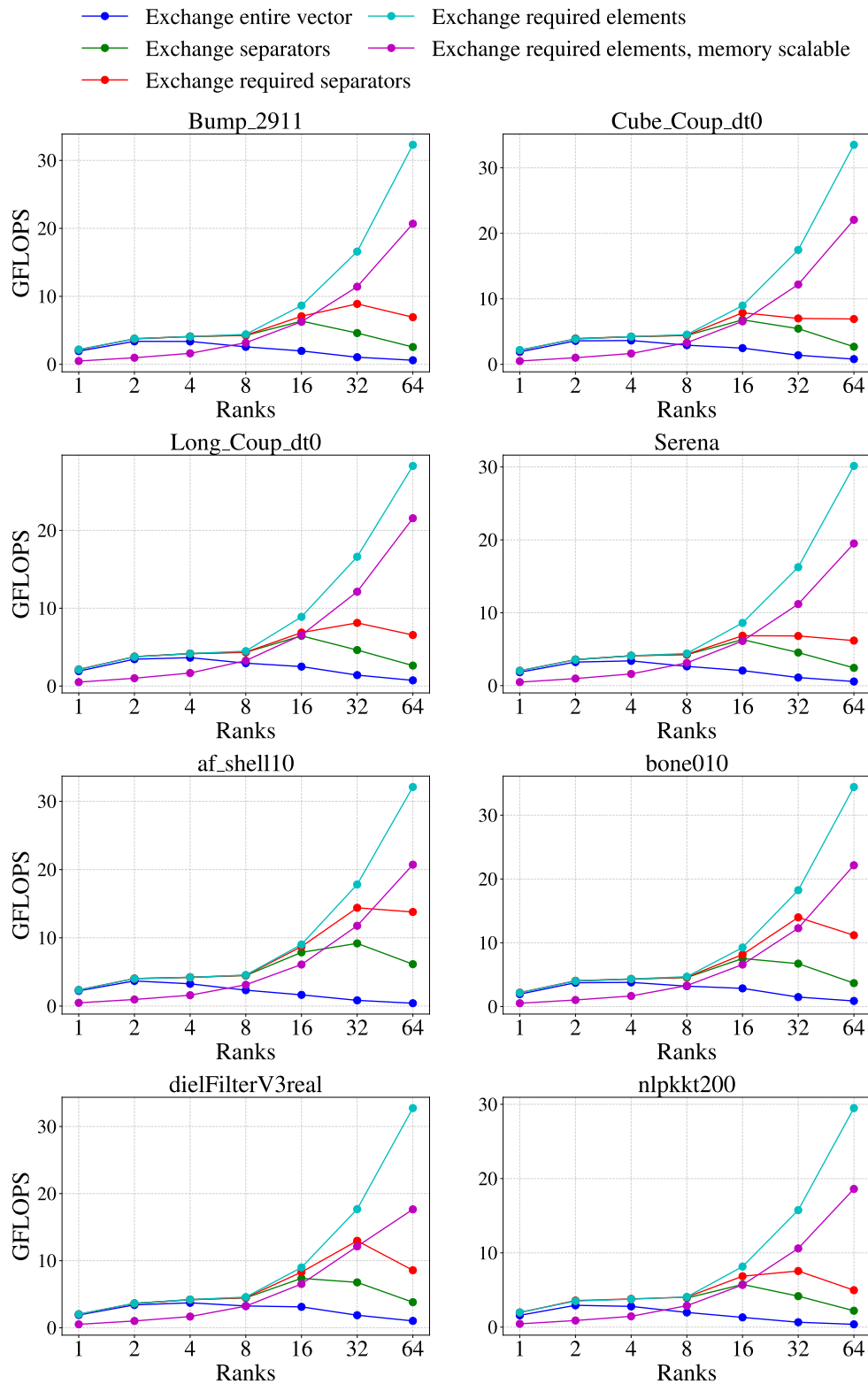


Figure 5.2: Single Node - AMD EPYC 7601

Figure 5.2 presents the achieved GFLOPS for each communication strategy. The performance trends largely align with expectations: each successive strategy generally exhibits improved performance over its predecessor. However, an exception arises with strategy E, which consistently underperforms relative to strategy D.

As discussed in section 4.5, strategy E reorders the local vector and separators. The effect this reordering has on well ordered matrices is that it most likely reduces the amount of cache reuse. This has not been measured directly, but it is the most likely culprit to the discrepancy between the results of strategy D and E.

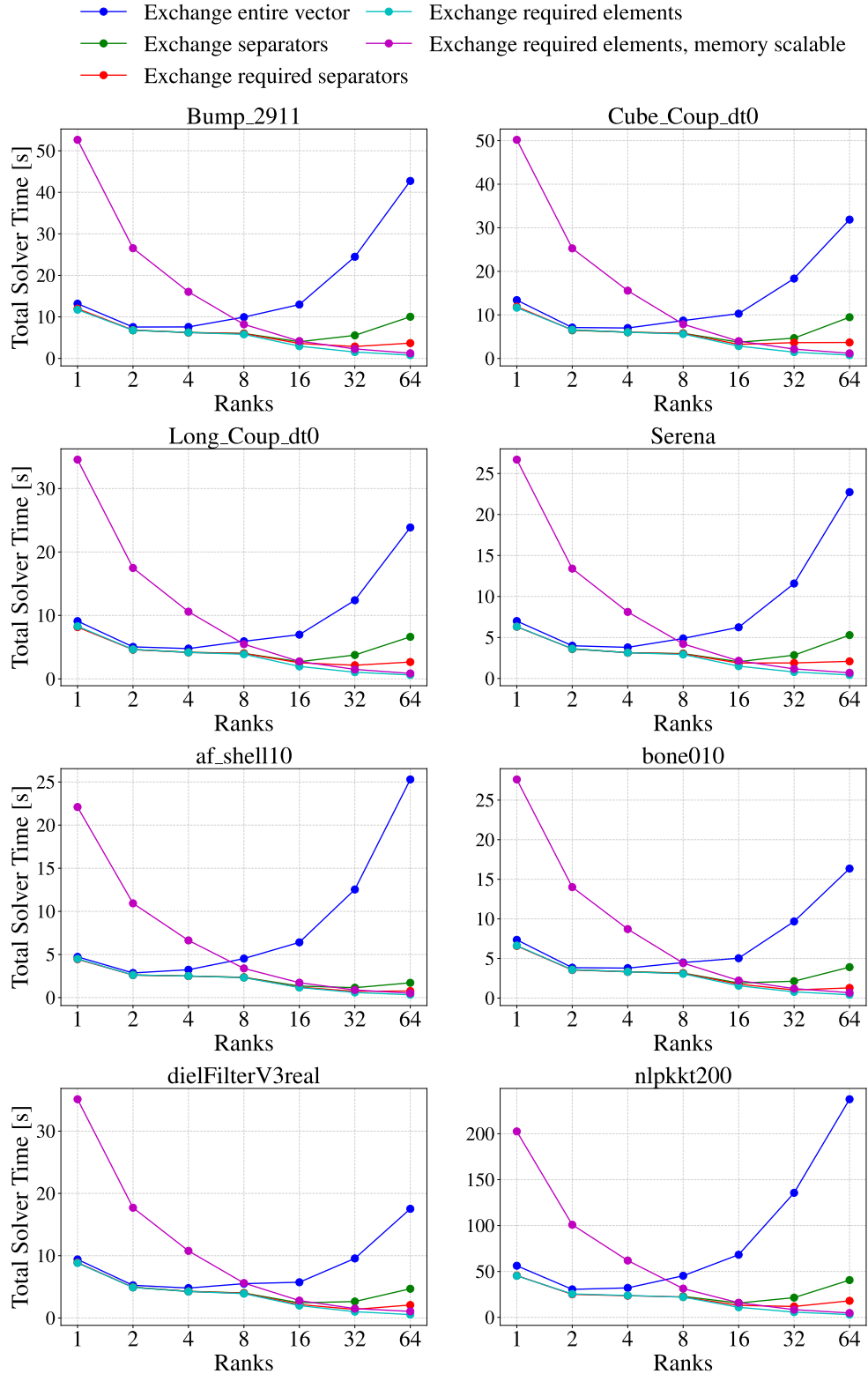


Figure 5.3: Total execution time of each communication strategy on a single node using the AMD EPYC 7601 chip.

Figure 5.3 presents the total execution time for each communication strategy. It is closely related to Figure 5.2, as computing the GFLOPS number is given by 5.2.

$$\text{GFLOPS} = \frac{\text{No. of flops performed}}{\text{Total execution time}} \quad (5.2)$$

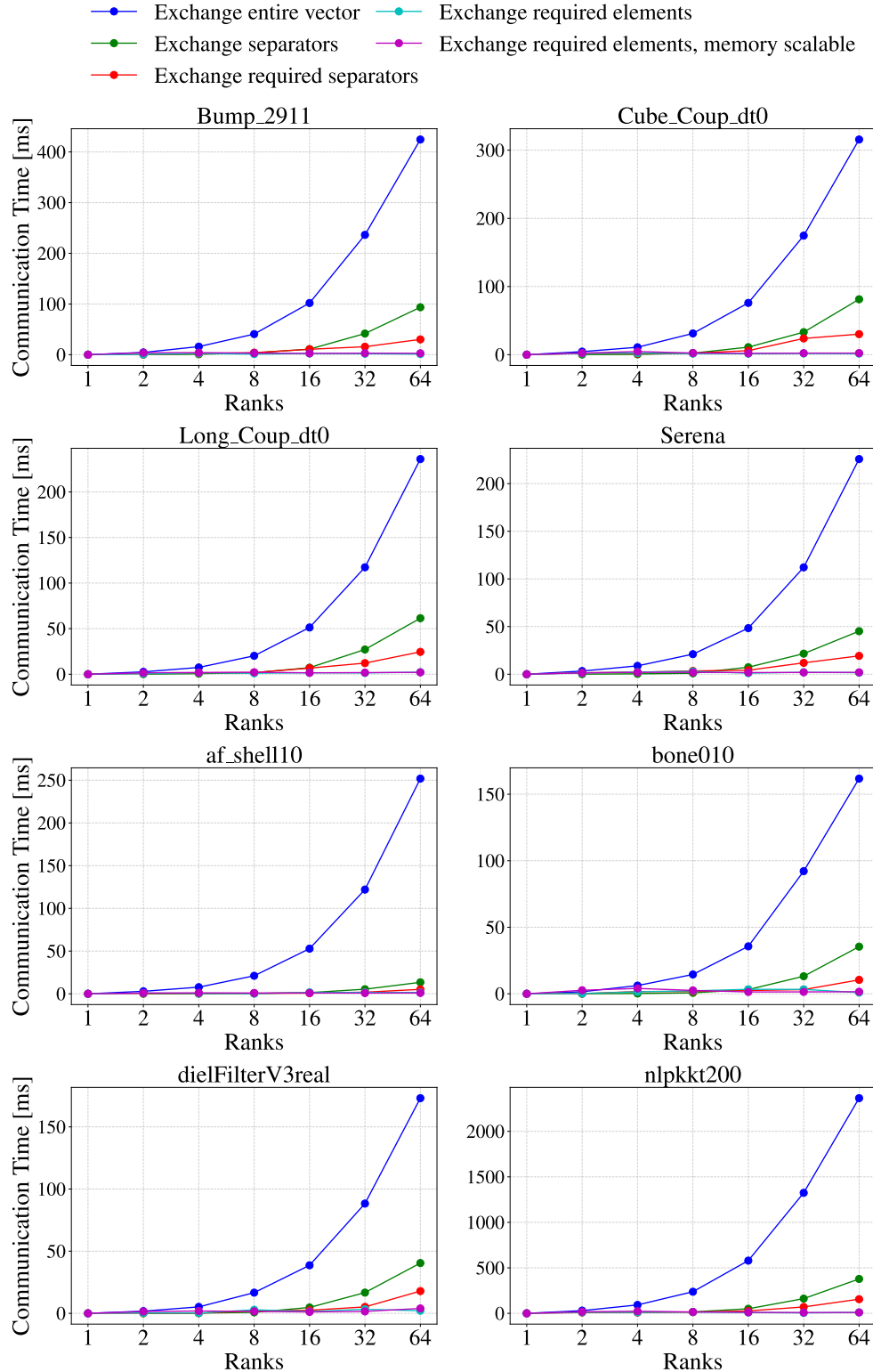


Figure 5.4: Communication time component of each strategy on a single node using the AMD EPYC 7601 chip.

Figure 5.4 present the time spent performing intra-node communication for each iteration of SpMV. The results clearly illustrate the performance benefits of optimizing communication in distributed single node SpMV. Strategy A acts as a baseline, by naively communicating the entire vector. Each successive communication strategy implements measures to reduce the communication volume, and it can be seen that this does indeed result in lower communication times. Strategy B limited communication to communicating only separators, Strategy C narrowed this to only communicating the separators to the rank that need them. Finally, strategy D and E further reduces the communication volume by only communicating necessary separator elements. This progression confirms the role communication strategies play in reducing the bottleneck that the data-dependencies between nodes induce. The results emphasize that careful attention to communication minimization yields improvements communication time, and by extension in performance for memory-bound operations like SpMV.

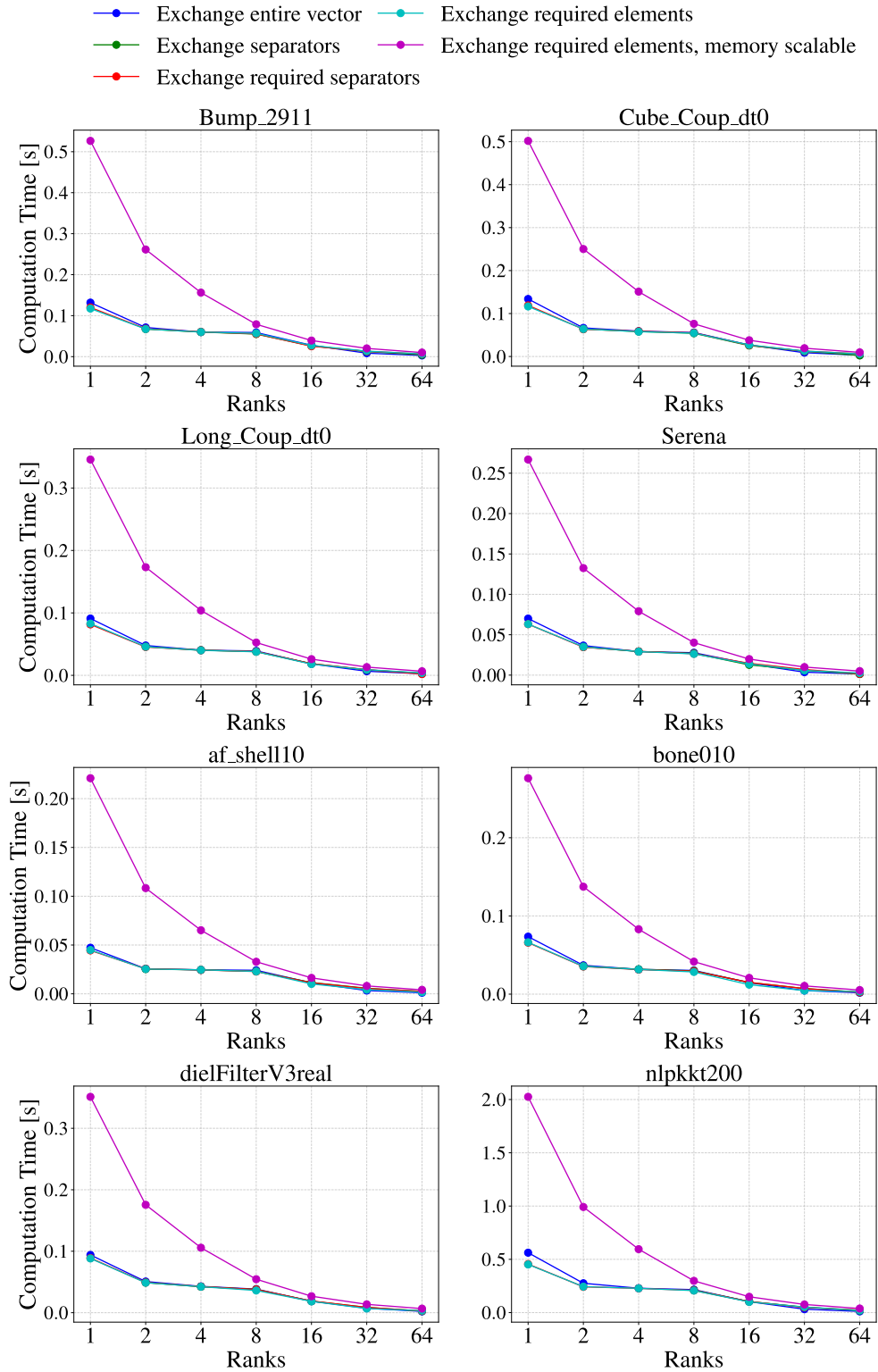


Figure 5.5: Computation time component of each strategy on a single node using the AMD EPYC 7601 chip.

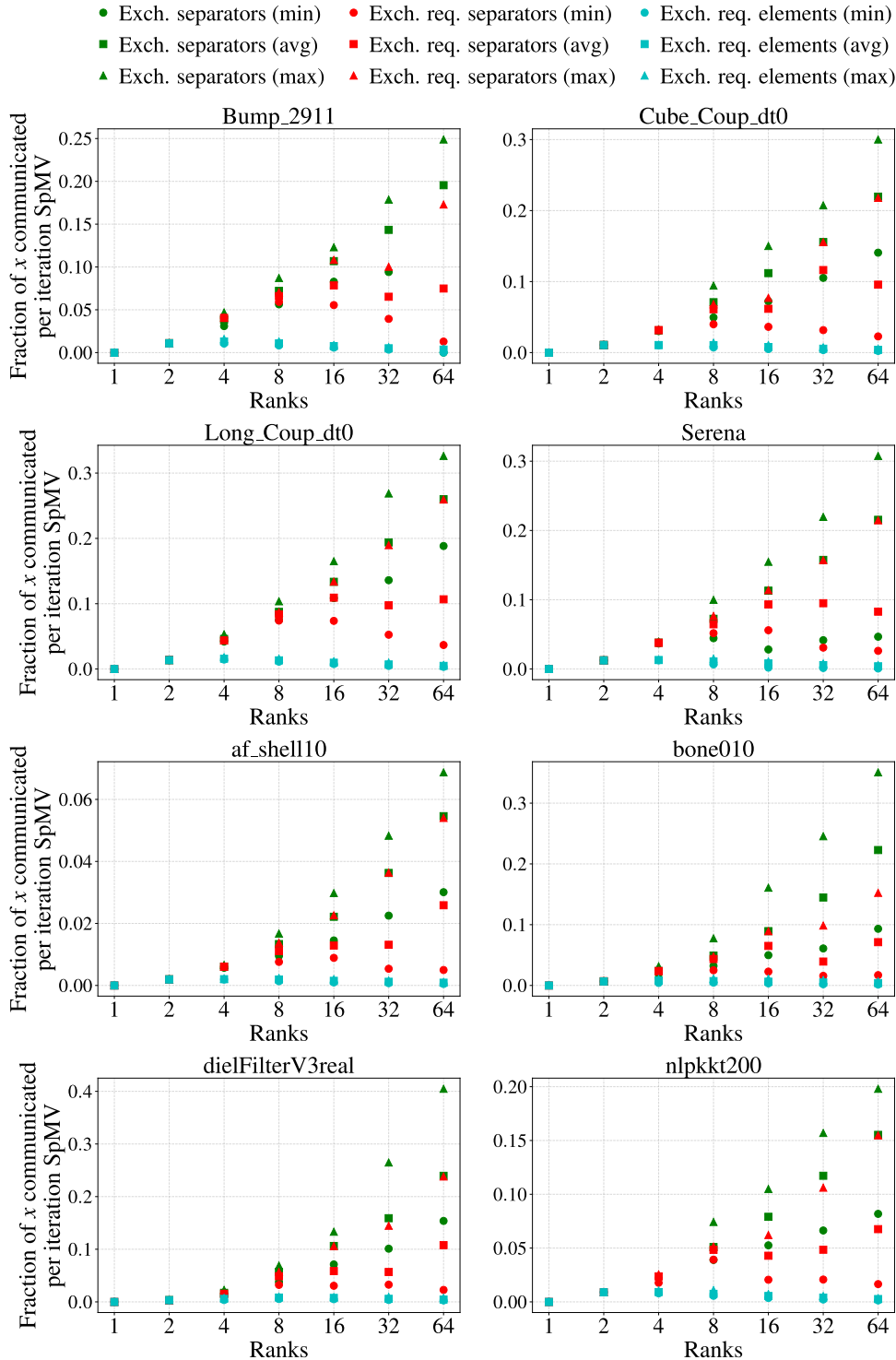


Figure 5.6: Fraction of x communicated per SpMV iteration each strategy on a single node using the AMD EPYC 7601 chip.

Figure 5.6 shows the fraction of the input vector x communicated per SpMV iteration across various matrices and ranks for different communication strategies. This figure provides an important quantitative counterpart to the timing data: it confirms that strategies which yielded lower communication time also effectively minimized the volume of communicated data. The results presented in this figure only show the communication volume for strategies B-D. Strategy A have been left out as the fraction of x communicated in each iteration is 1 no matter how many ranks are used. Strategy E has been left out as the communication volume for this strategy is the same as strategy D.

Notably, when comparing strategy B and C, the rank with the maximum communication volume in strategy C is usually equal to, or lower than the average communication volume of strategy B.

5.5 AMD EPYC 7601 - Multi Node Performance

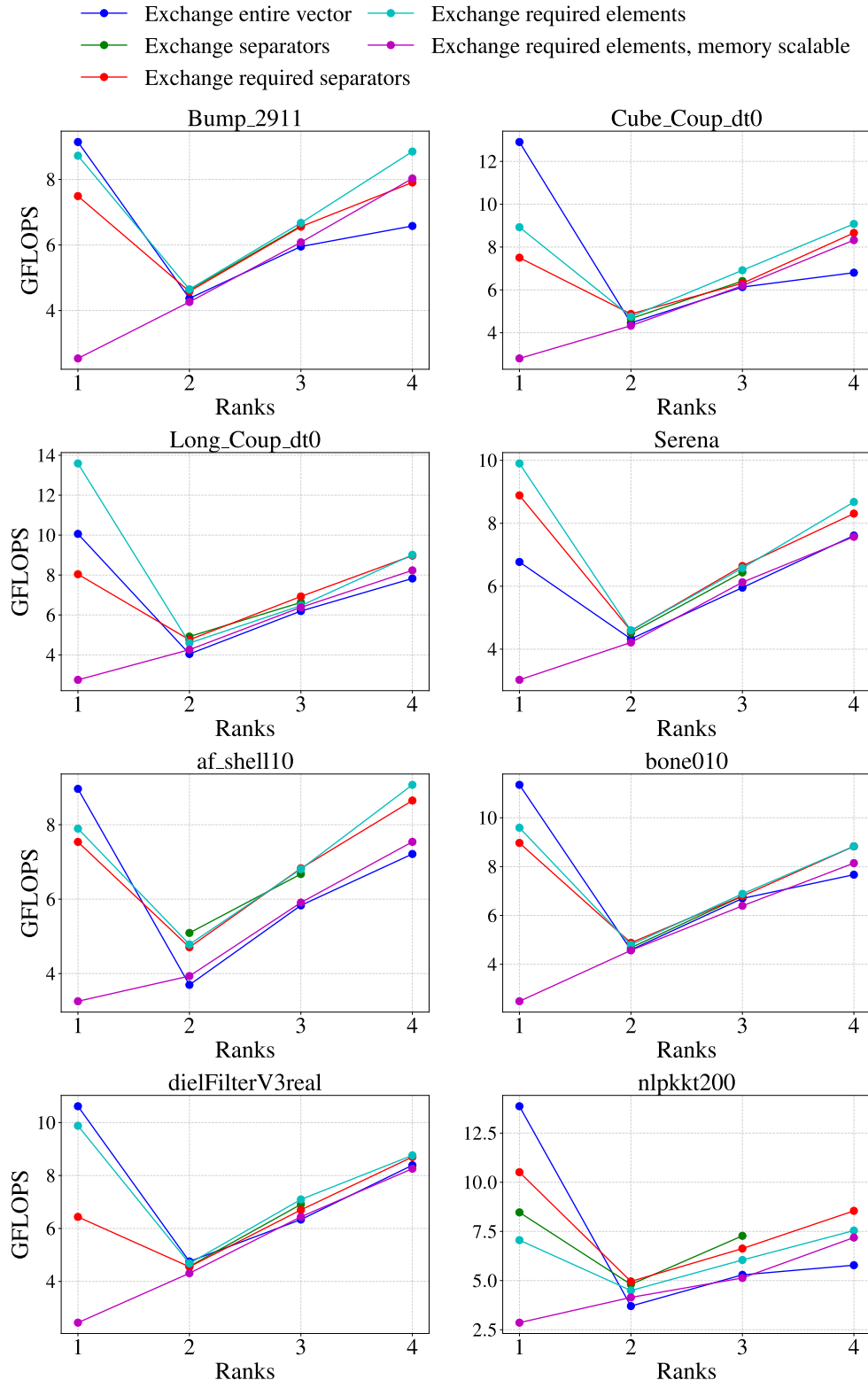


Figure 5.7: Achieved GFLOPS on multi node setup using the AMD EPYC 7601 chip.

The results presented in Figure 5.7 illustrate the GFLOPS achieved when running SpMV for 100 iterations in a distributed and shared memory hybrid environment. For these results, 4 nodes running dual-socketed AMD EPYC 7601 chips have been used, with one MPI rank placed on each node. The results largely align with what is expected, as each consecutive communication strategy outperforms the previous.

The results illustrate some quirks that are inherent to the AMD EPYC 7601 chip. As is evident from the plots, using only one node (and one MPI rank), consistently yield results that are either better or almost as good as the results achieved when using the maximum amount of available nodes. As an example, for the Bump_2911 matrix, strategy D achieves a GFLOPS performance of ≈ 9 GFLOPS on one node, with 64 OpenMP shared memory threads. When this is compared to Figure 5.2 using 64 MPI ranks, which achieves ≈ 30 GFLOPS for the same matrix. It is clear that using only distributed memory far outperforms using only shared memory parallelization. The reasons for this is outside the scope of this thesis, but the AMD EPYC 7601 chip is a 1st generation chip, and does have a weak core to core connection, which could be the reason.

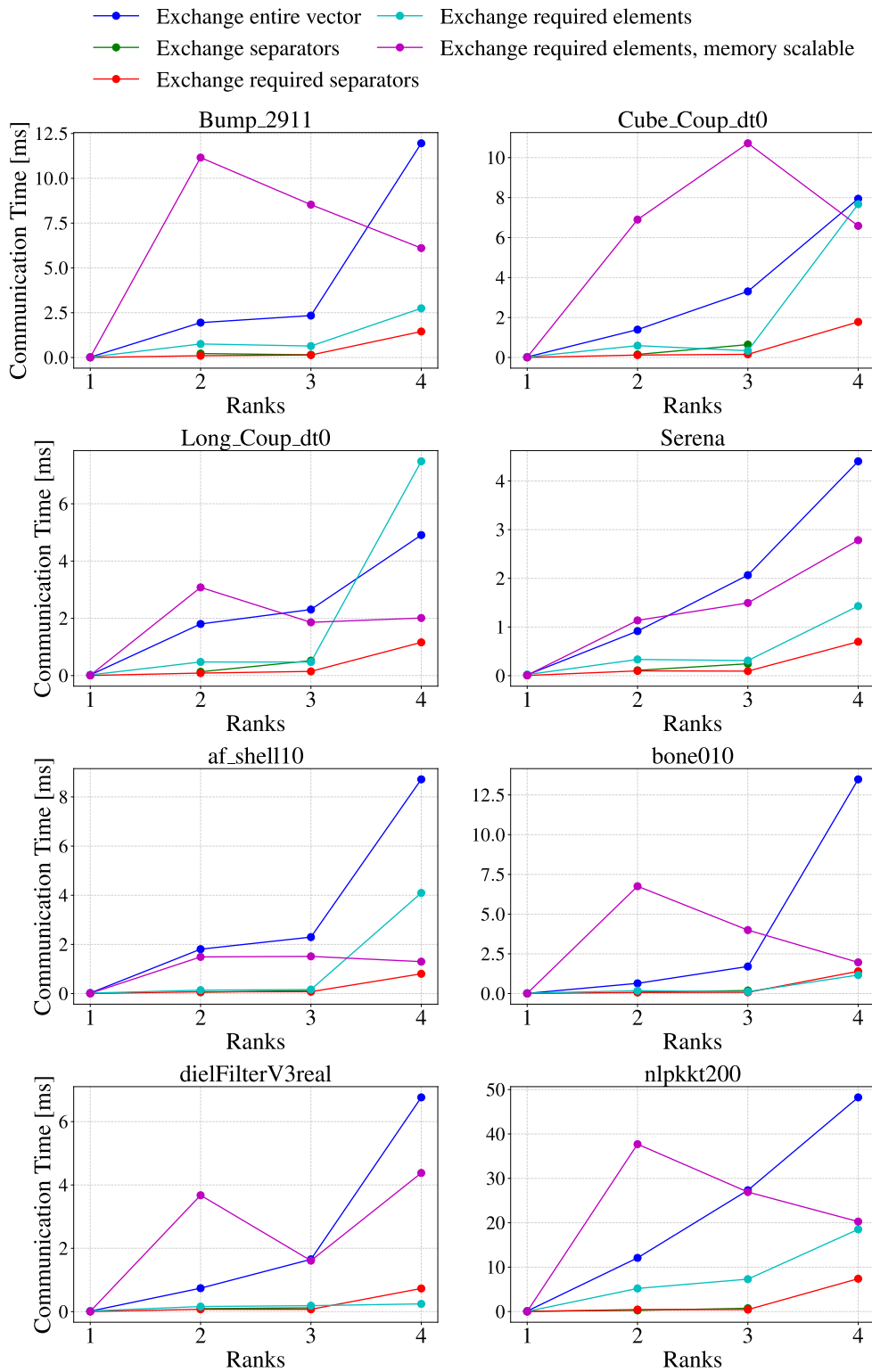


Figure 5.8

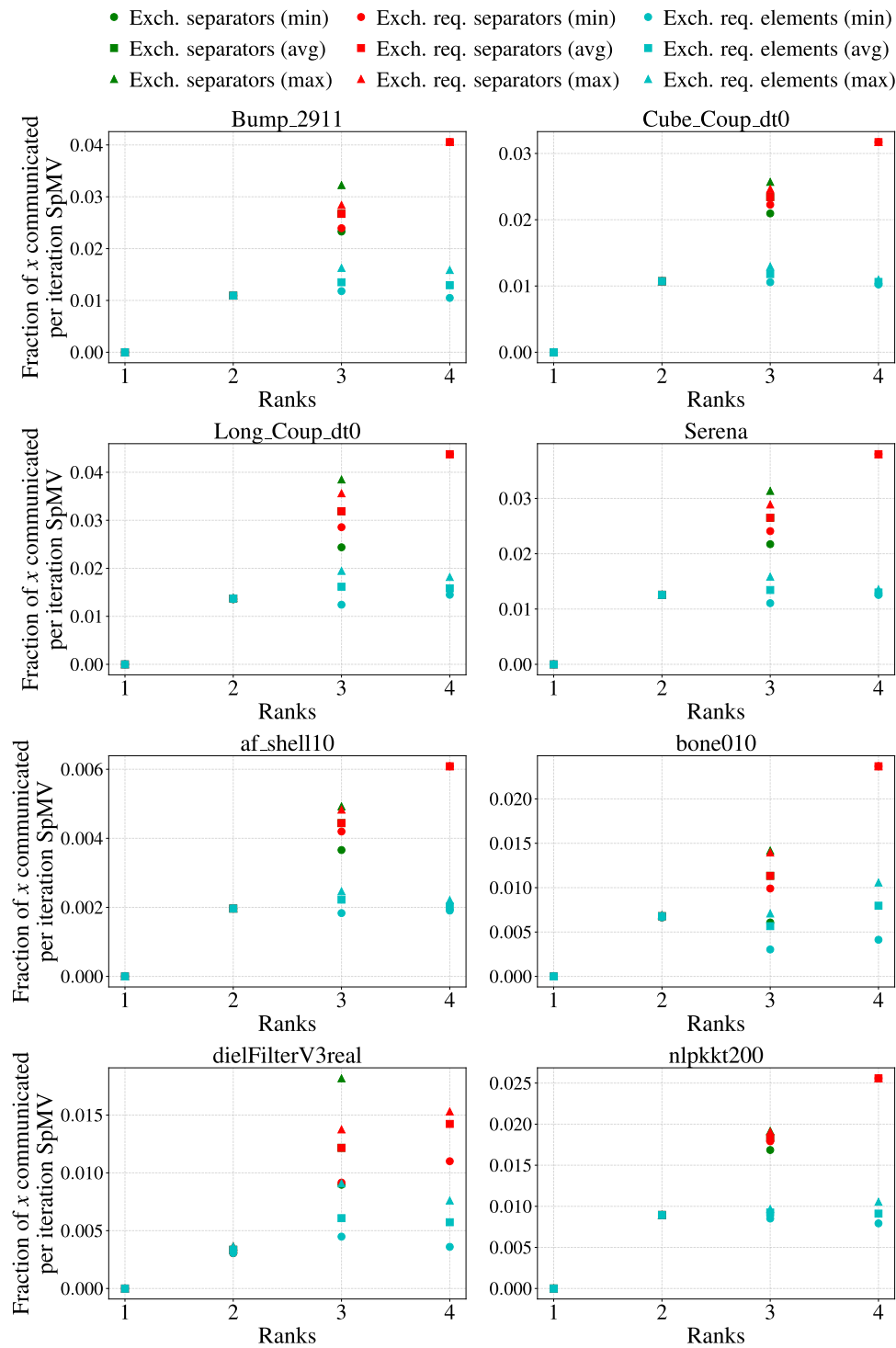


Figure 5.9

5.5.1 2 proc per node

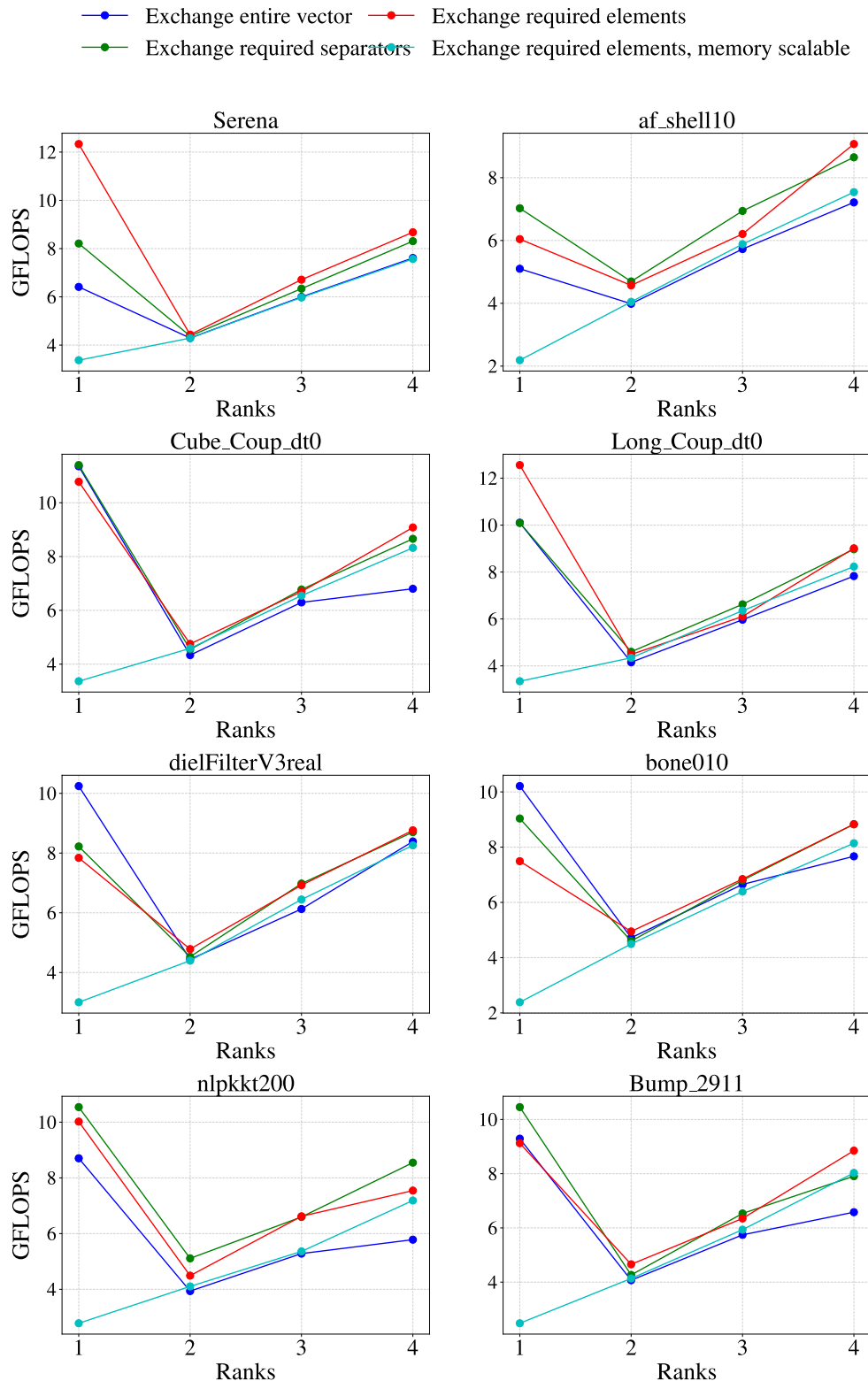


Figure 5.10: Multi Node - AMD EPYC 7601

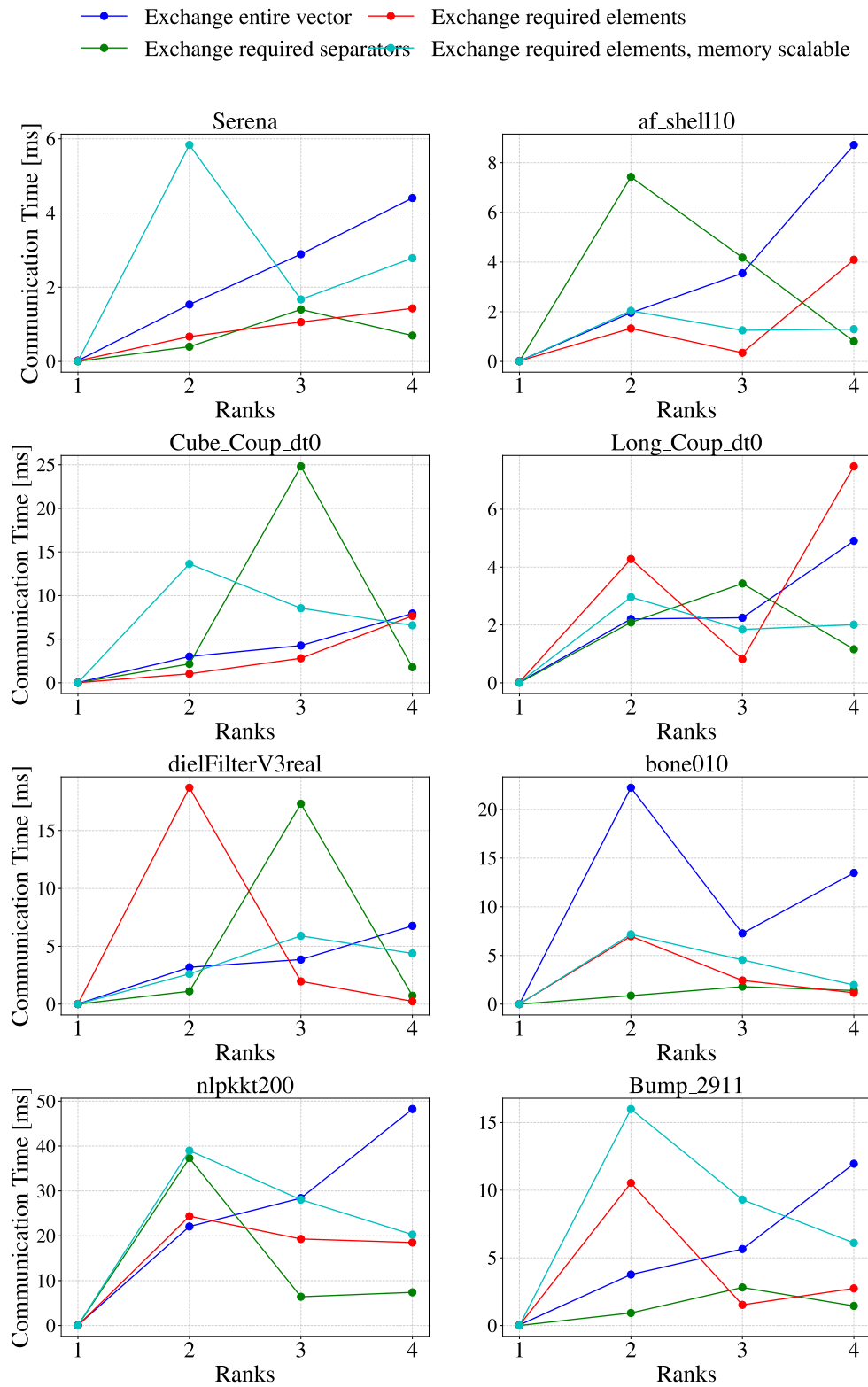


Figure 5.11

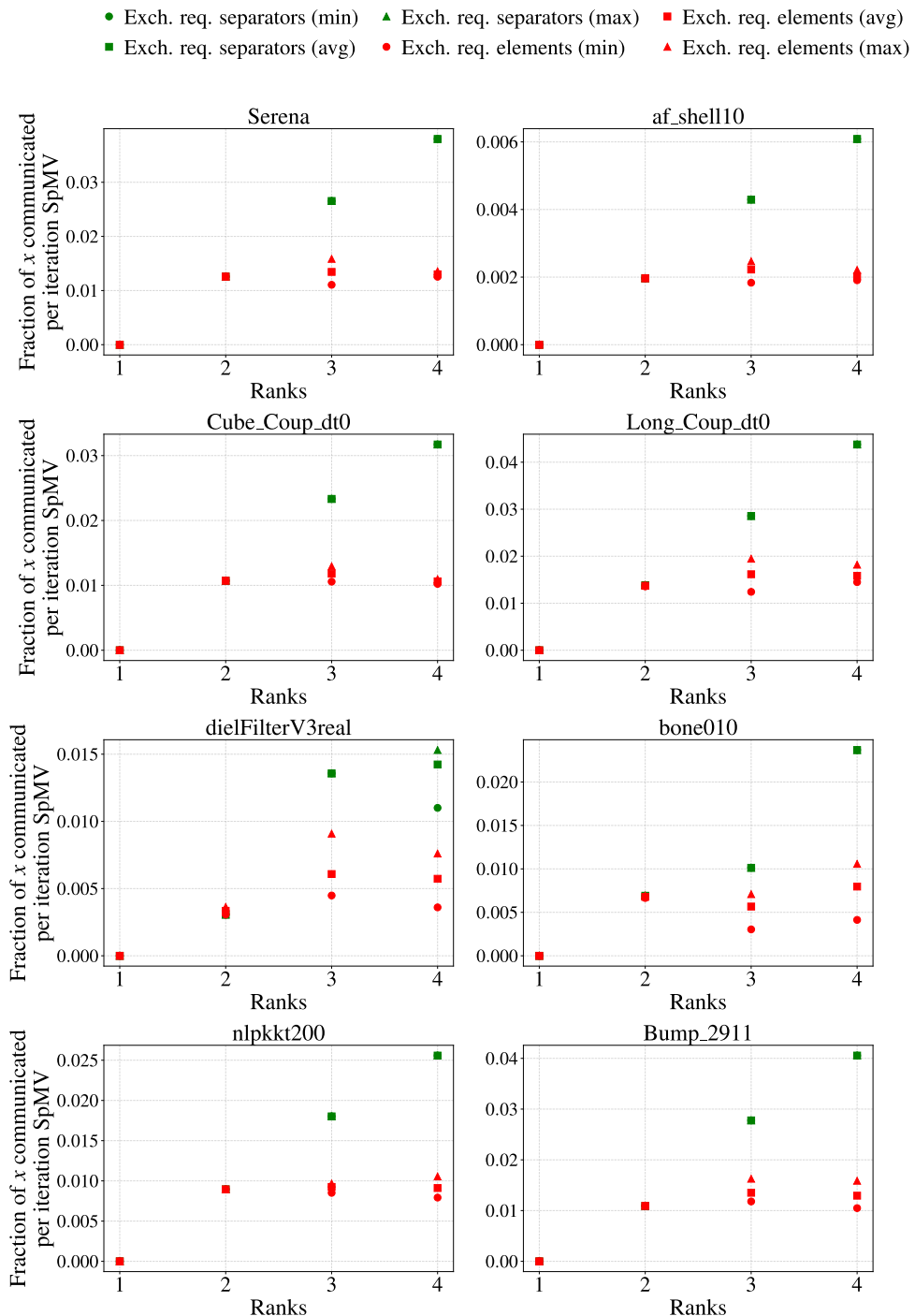


Figure 5.12

5.6 AMD EPYC 7302P - Multi Node Performance

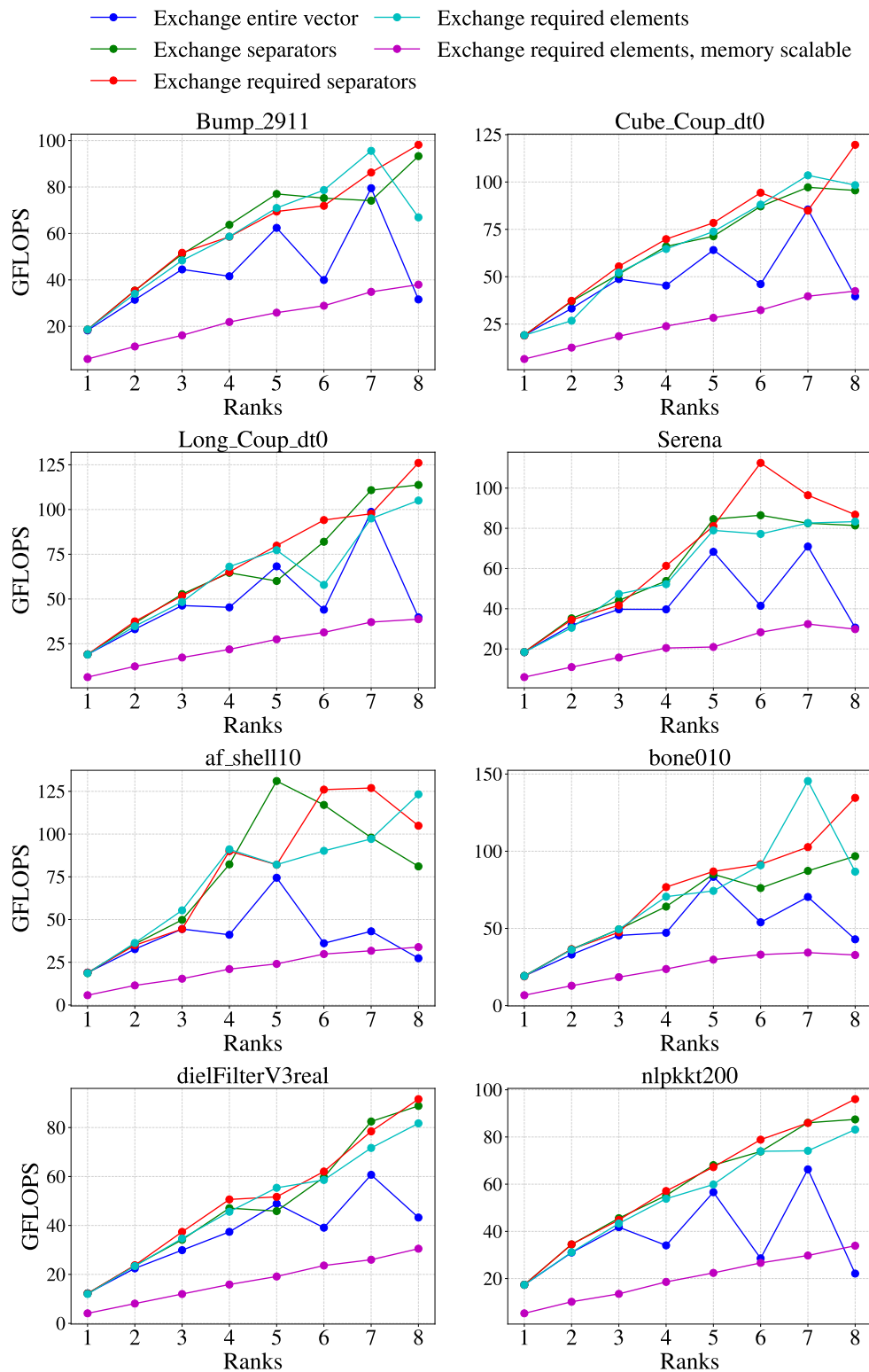


Figure 5.13: Achieved GFLOPS on multi node setup using the AMD EPYC 7302P chip.

Figure 5.13 illustrates the achieved GFLOPS on up to 8 single socketed nodes using the AMD EPYC 7302P chip. Notice how strategy A exhibits a "zig-zag" pattern depending on whether or not the number of nodes is even or odd. This is due to a quirk of how MPI decides to work (see [10]).

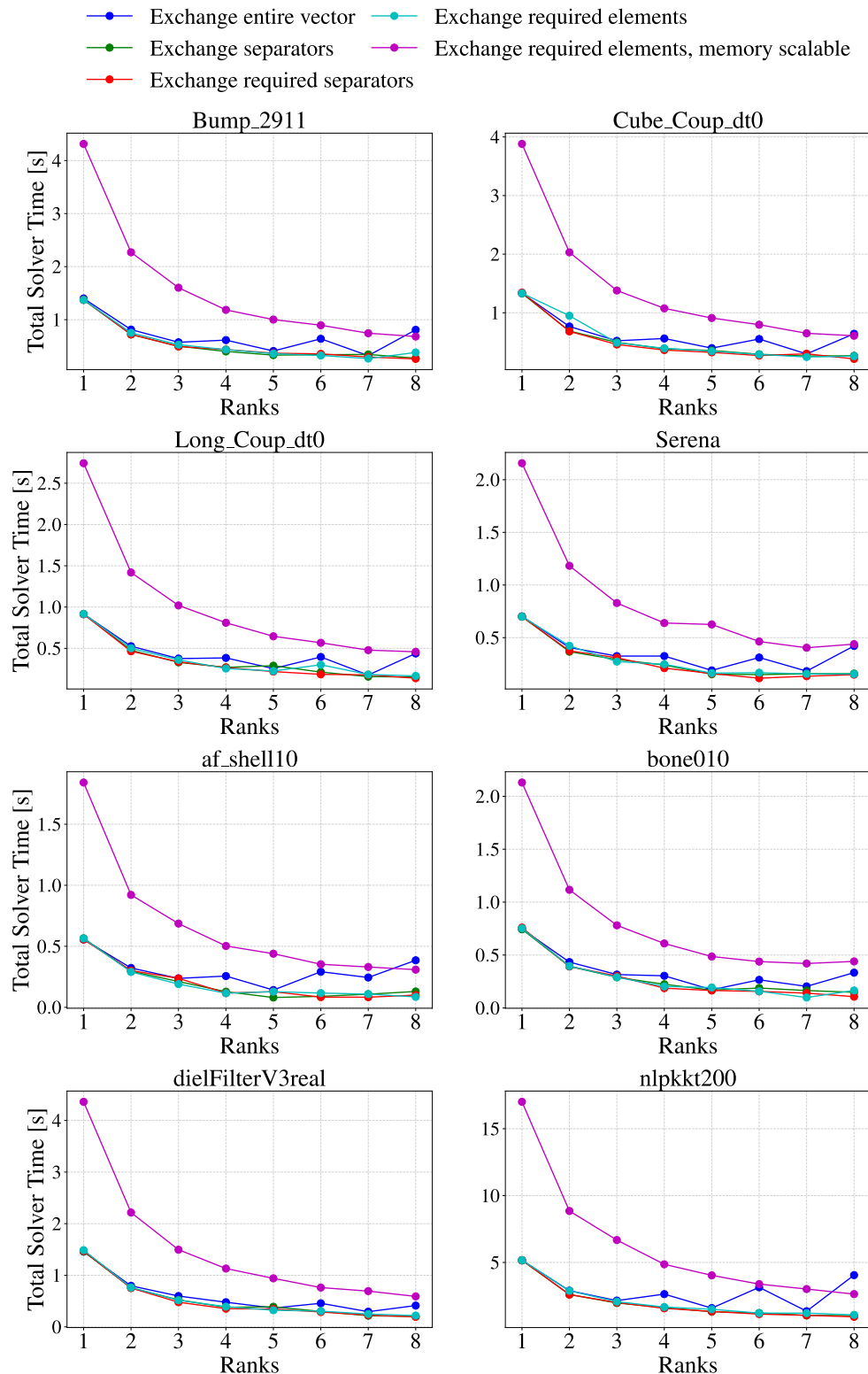


Figure 5.14

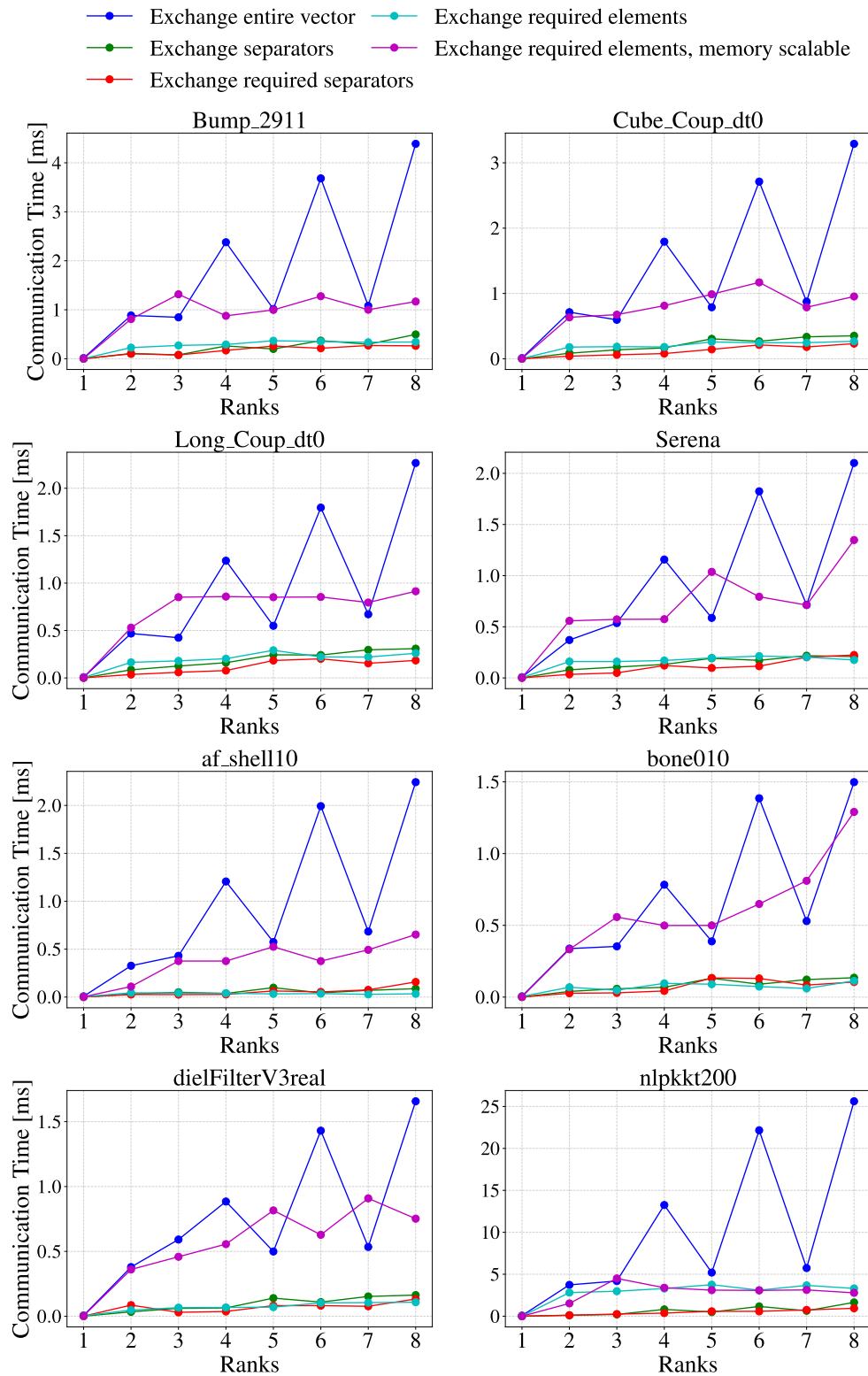


Figure 5.15

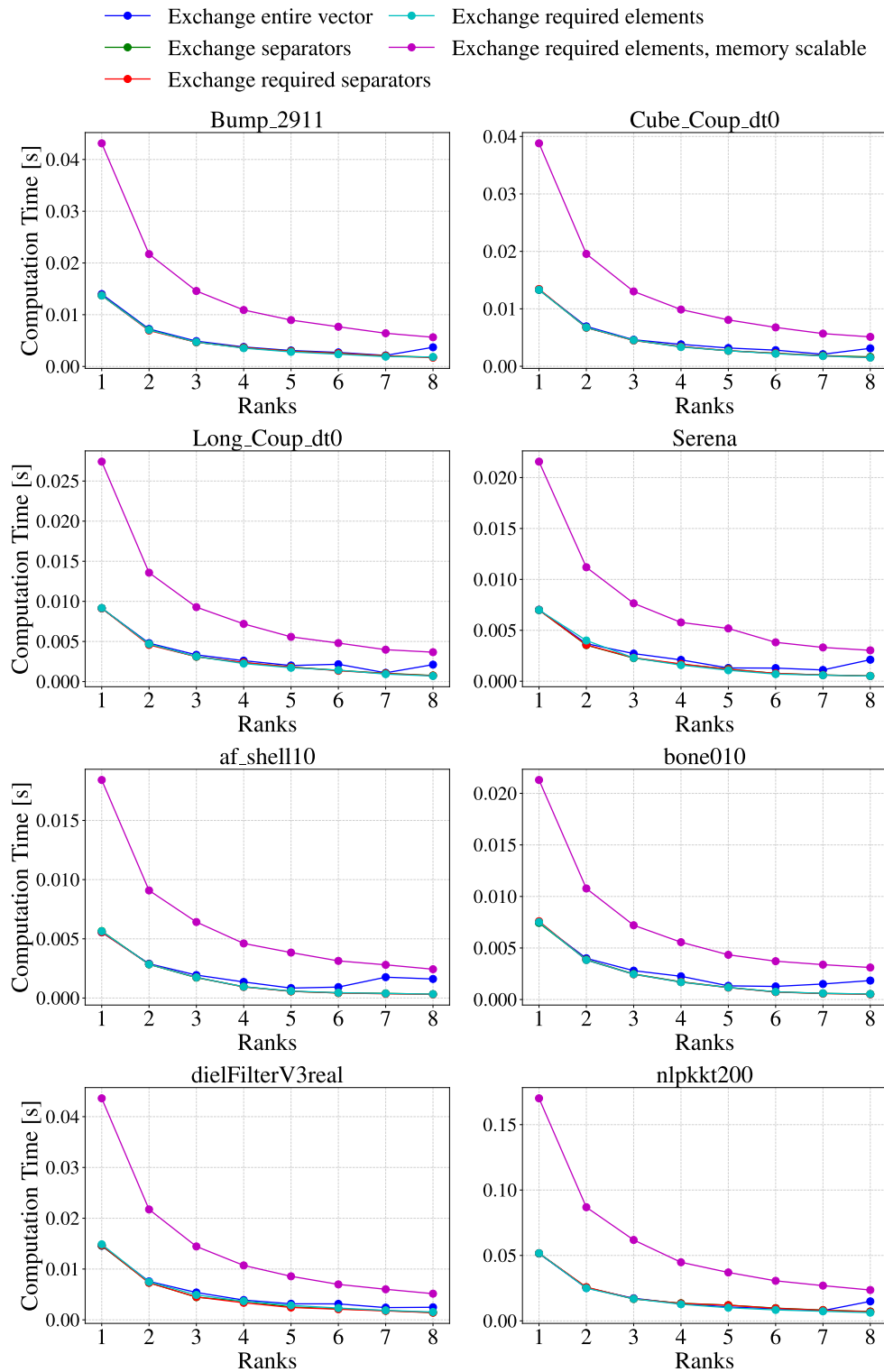


Figure 5.16: Tcomp 2X4 Multi Rome16Q

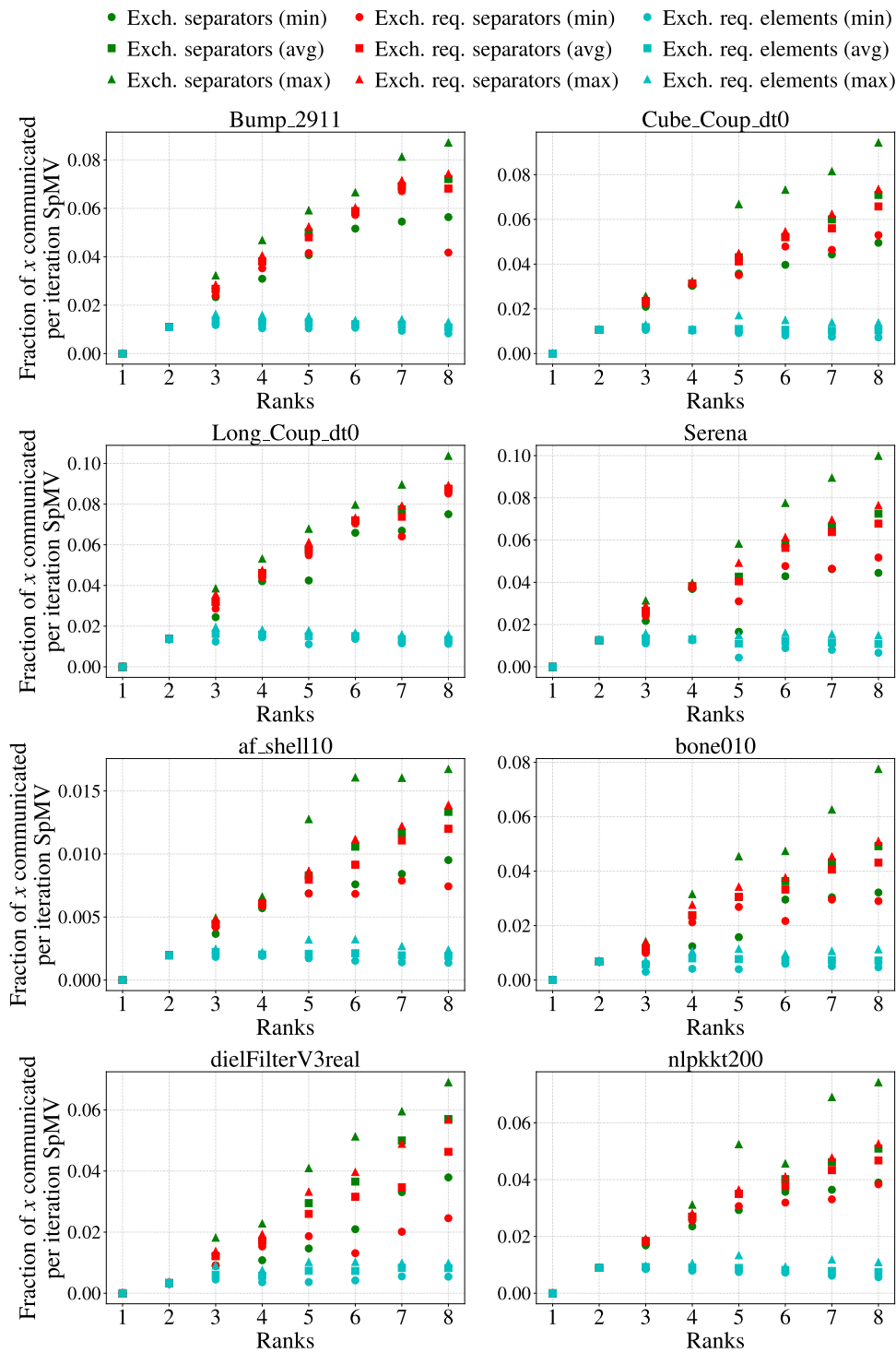


Figure 5.17

5.7 AMD EPYC 7413 - Multi Node Performance

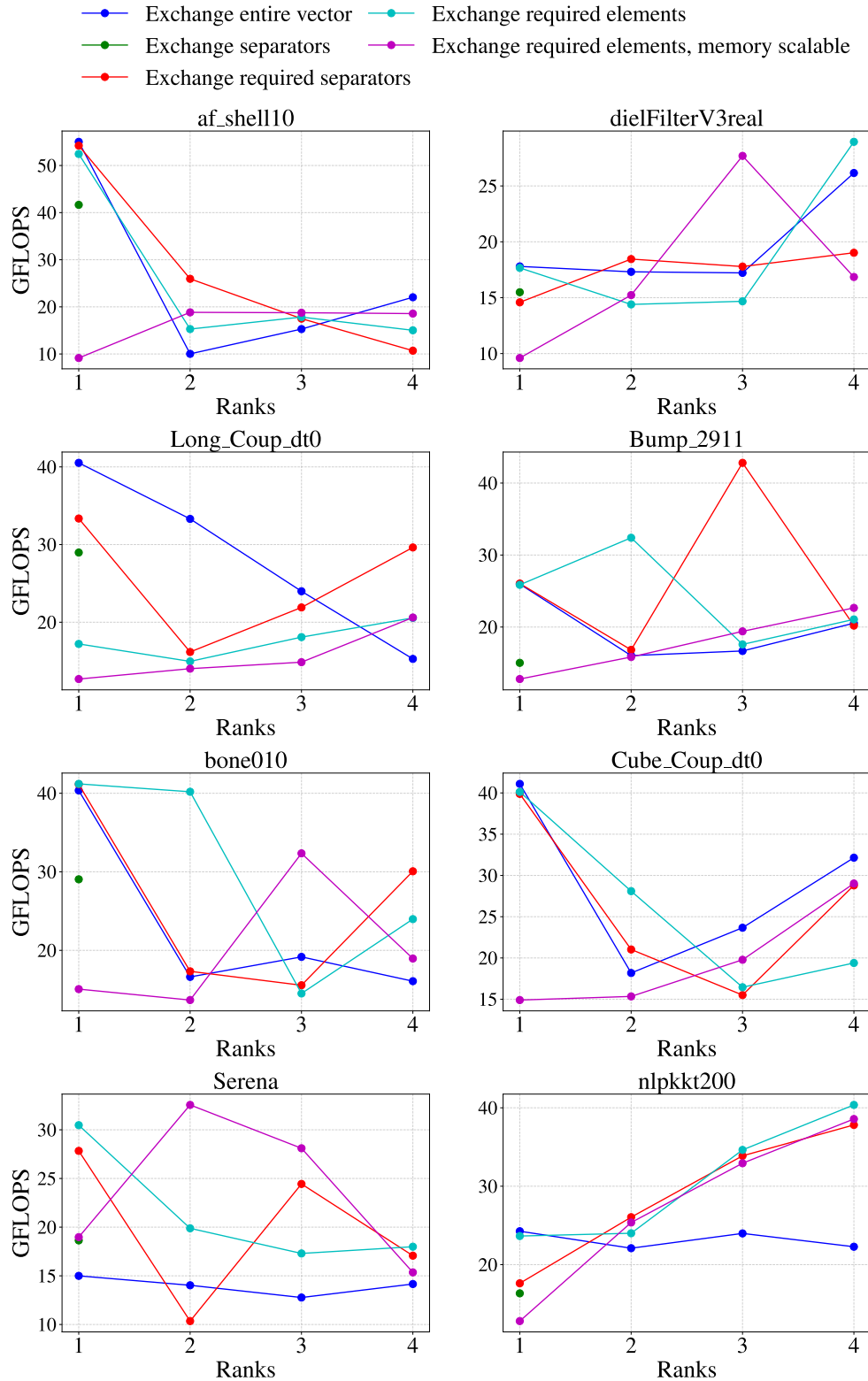


Figure 5.18: multi Node - AMD EPYC 7413

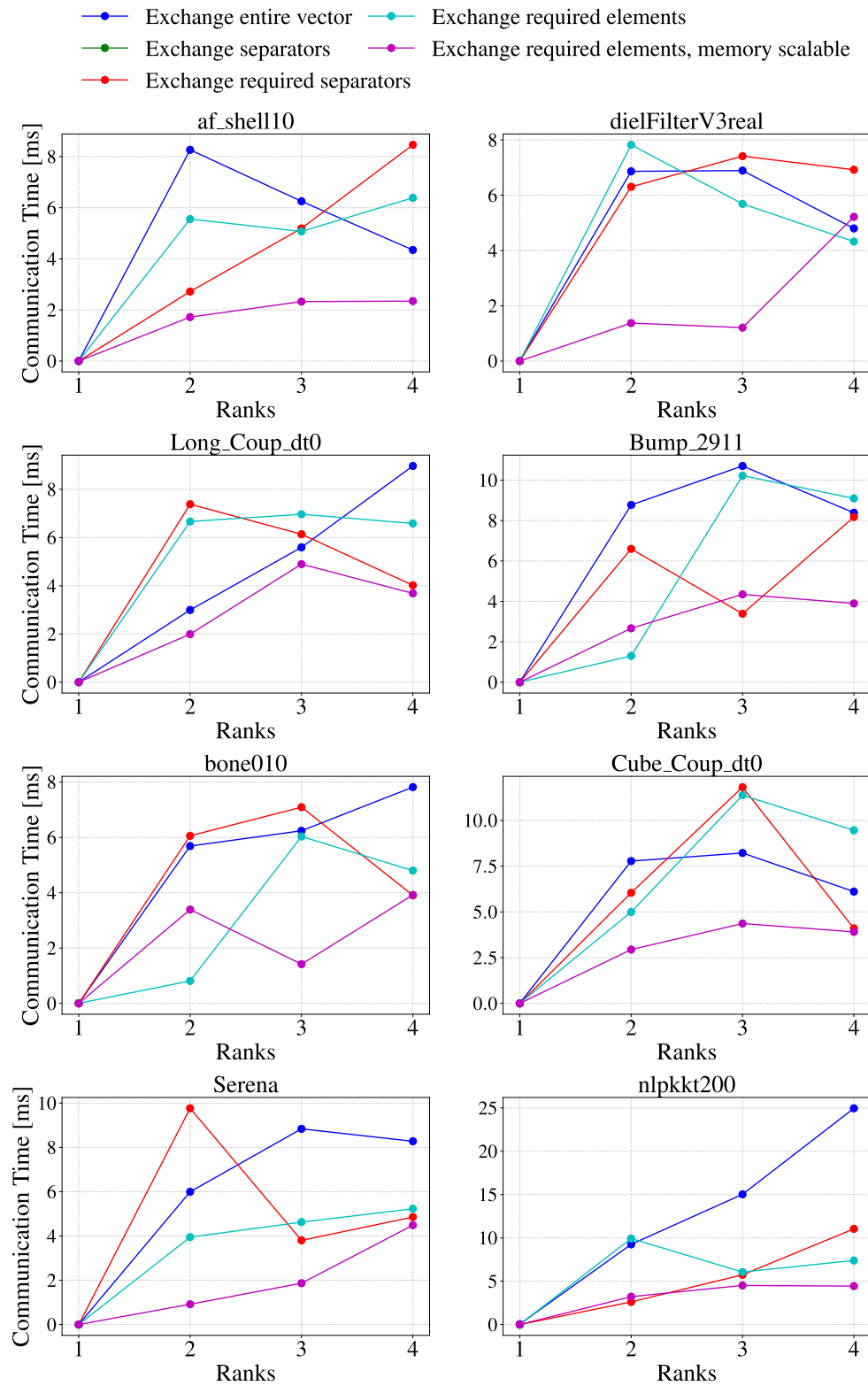


Figure 5.19

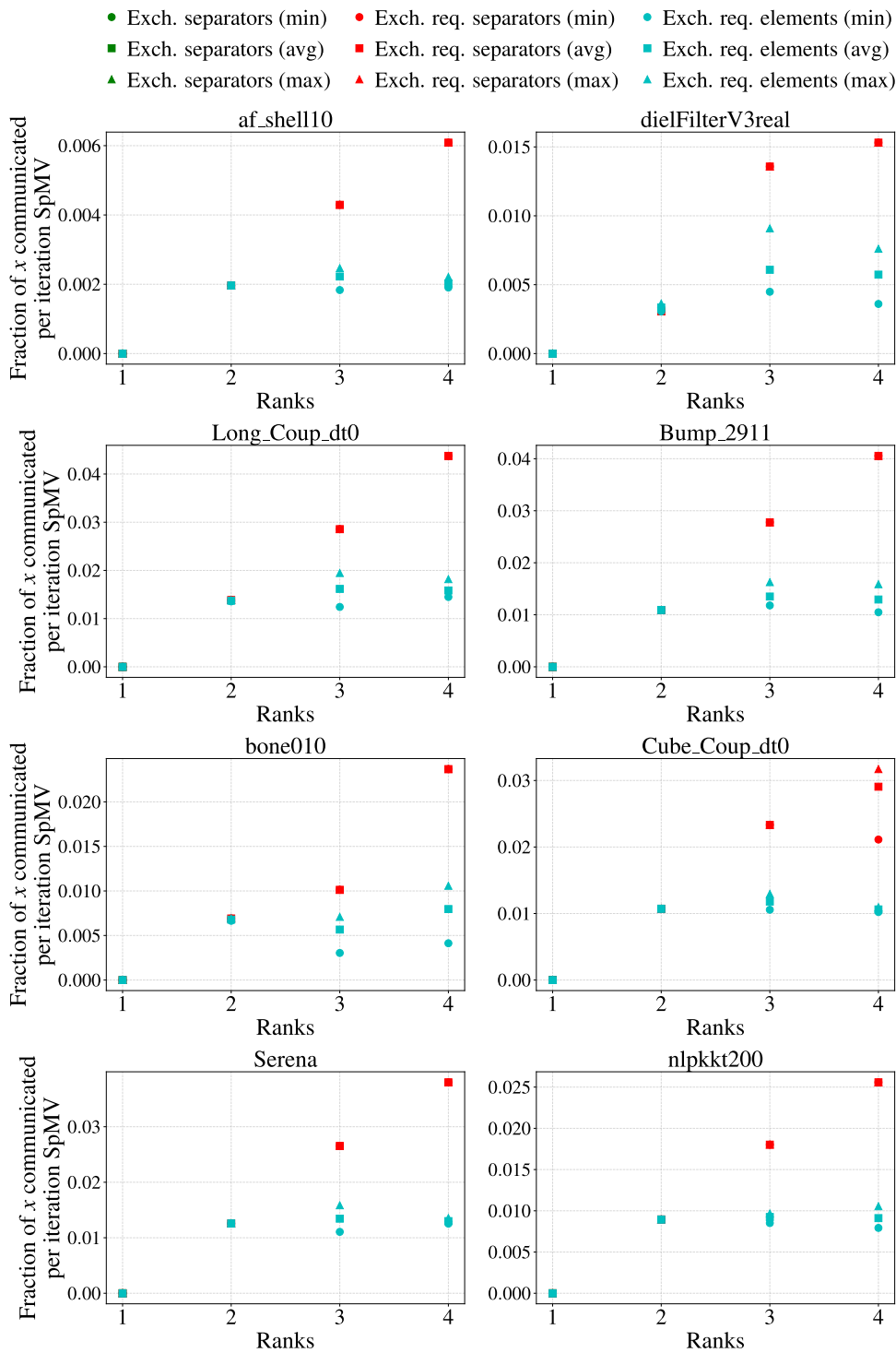


Figure 5.20

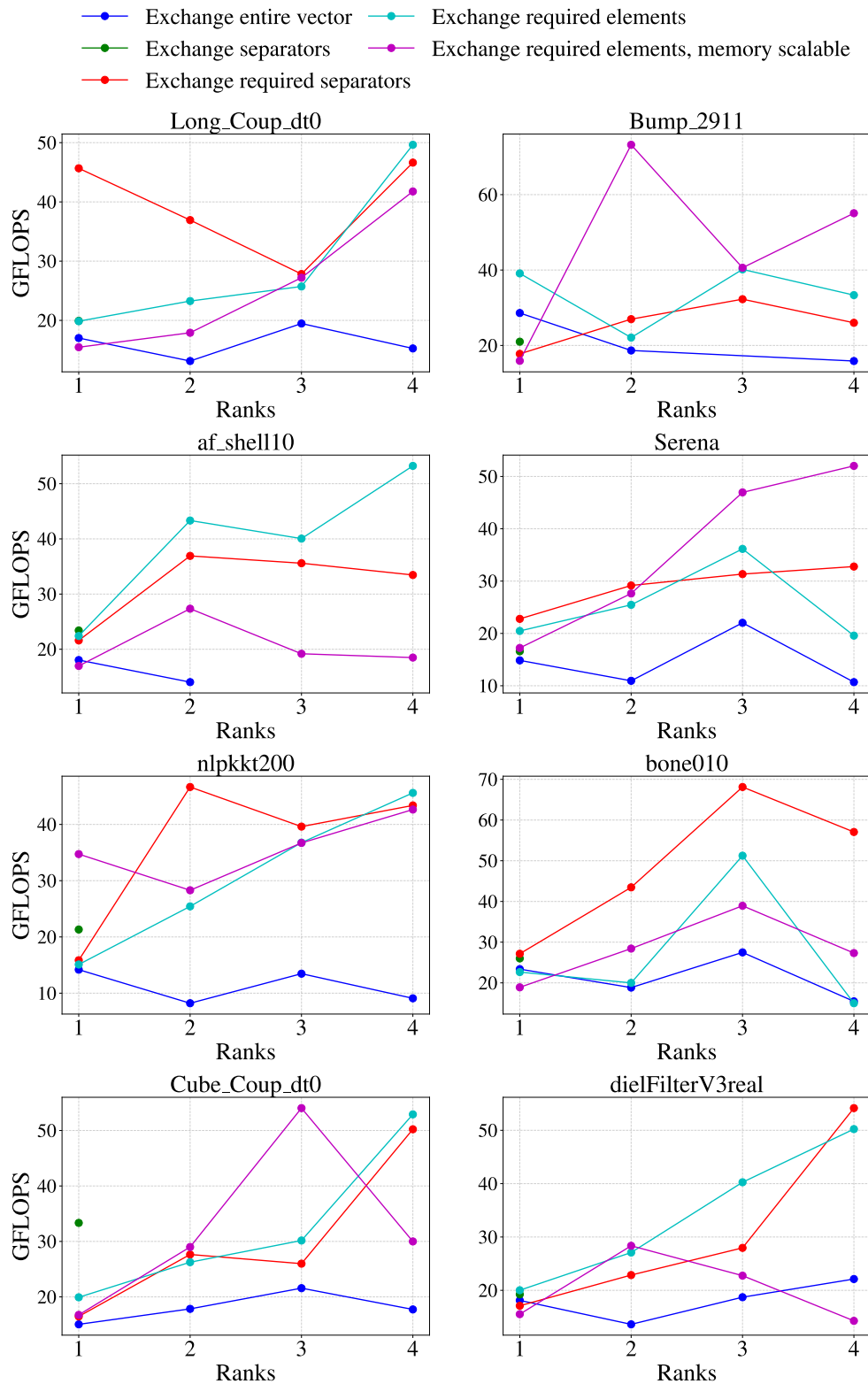


Figure 5.21: Multi Node - AMD EPYC 7413

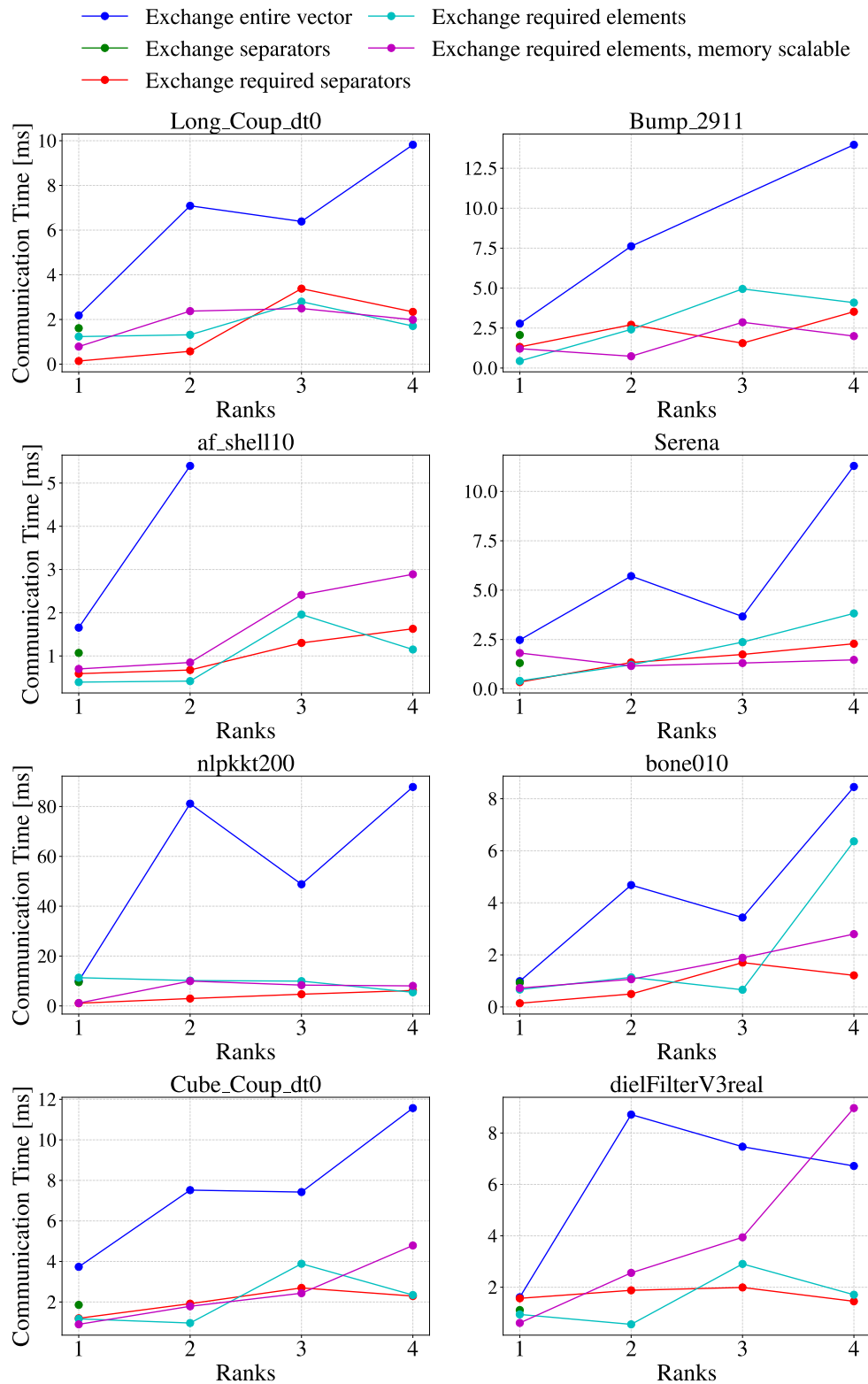


Figure 5.22

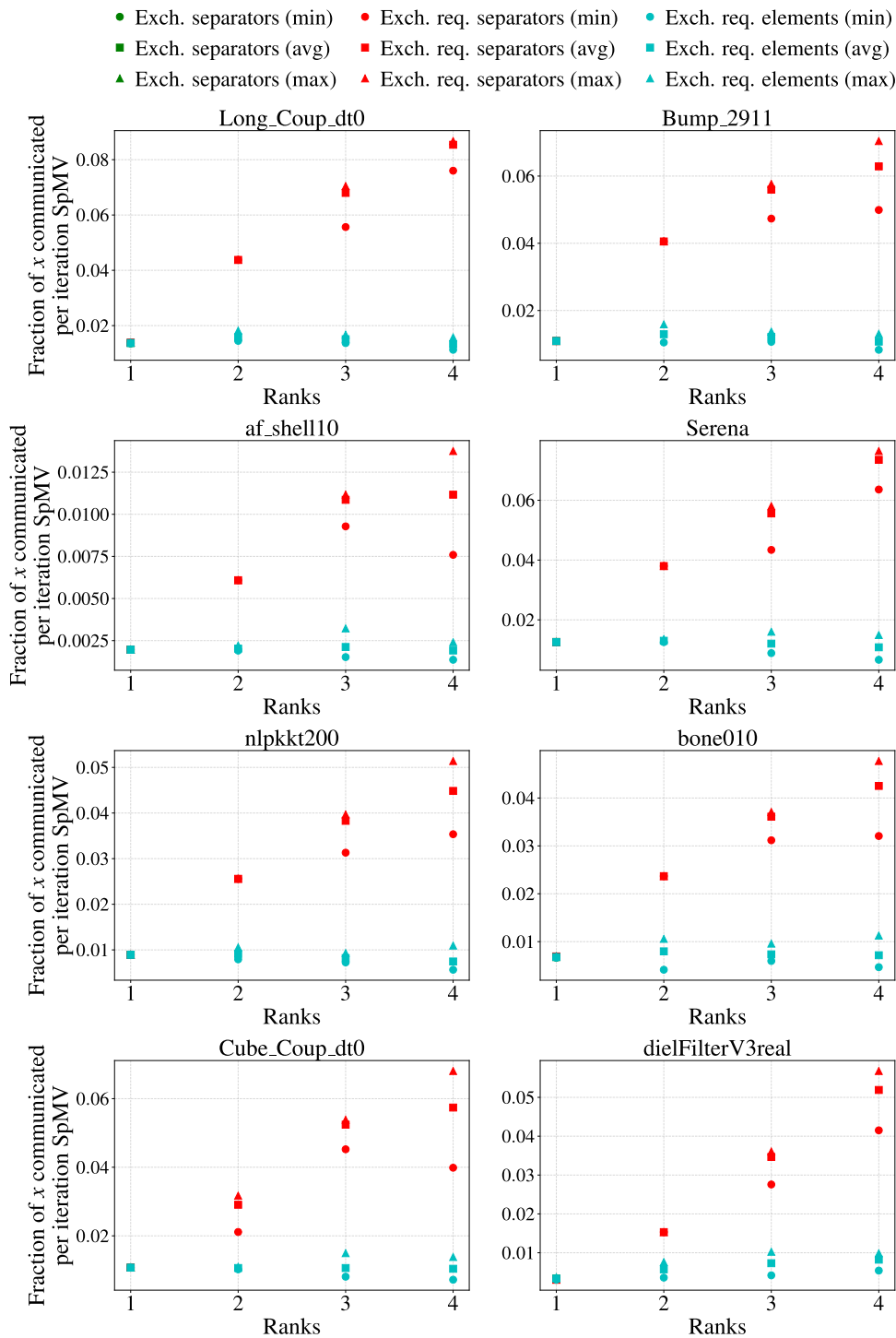


Figure 5.23

Table 5.1: Hardware used in our experiments. STREAM Triad was run with the `-march=native` and `-O3` compilation flags.

	Xeon-A	FPGAQ	Naples	Rome	Milan	TX2	Hi1620
CPUs	Intel Xeon Gold 6130	AMD Epyc 7413	AMD Epyc 7601	AMD Epyc 7302P	AMD Epyc 7763	Cavium TX2 CN9980	HiSilicon Kunpeng 920-6426
Instr. set	x86-64	x86-64	x86-64	x86-64	x86-64	ARMv8.1	ARMv8.2
Microarch.	Skylake	Zen 3	Zen	Zen 2	Zen 3	Vulcan	TaiShan v110
Sockets	2	2	2	1	2	2	2
Cores	2×16	2×24	2×32	1×16	2×64	2×32	2×64
Freq. [GHz]	1.9–3.6	2.6–3.6	2.7–3.2	1.5–3.3	2.5–3.5	2.0–2.5	2.6
L1I/core [KiB]	32	64	64	32	32	32	64
L1D/core [KiB]	32	32	32	32	32	32	64
L2/core [KiB]	1024	512	512	512	512	256	512
L3/socket [MiB]	22	128	64	16	256	32	64
Mem. channels	2×6	2×8	2×8	1×8	2×8	2×8	2×8
Bandwidth [GB/s]	256	256(to be added)	342	204.8	409.6	342	342
Triad [GB/s]	147.1	137.4(to be added)	169.7	90.9	256.5	236.4	260.4

Chapter 6

Related Work

Merrill and Garland [8] propose a merge-based parallel SpMV algorithm that operates directly on the Compressed Sparse Row (CSR) format without requiring reformatting or auxiliary data structures. Their method employs a 2D merge-path decomposition that ensures strictly balanced workloads across processing elements, independent of row length variability. This design addresses the primary bottleneck of irregular row distributions in parallel SpMV, which often lead to performance inconsistencies in traditional row- and nonzero-splitting strategies. Evaluated across over 4,000 matrices, their approach demonstrated superior performance consistency and scalability, particularly on architectures with constrained local memories such as NUMA and GPUs. This work offers a compelling alternative to format-specific optimizations by achieving portability and high throughput directly on CSR representations.

Trotter et al. [11] present a comprehensive evaluation of matrix reordering strategies for enhancing sparse matrix-vector multiplication (SpMV) performance on multicore CPUs. Evaluating six reordering algorithms over 490 matrices on eight architectures, they find that reorderings based on graph and hypergraph partitioning (e.g., METIS, PaToH) offer the most consistent SpMV performance benefits. Their results indicate that performance improvements arise primarily from better data locality and reduced off-diagonal nonzero density, while bandwidth and profile reductions are less influential. They also underscore the architectural sensitivity of reordering effectiveness, suggesting that careful algorithm-architecture matching is critical. This study provides empirical validation for the effectiveness of reordering as a pre-processing optimization for SpMV, especially in shared-memory systems.

Bibliography

- [1] Luk Burchard, Kristian Gregorius Hustad, Johannes Langguth, and Xing Cai. Enabling unstructured-mesh computation on massively tiled ai processors: An example of accelerating in silico cardiac simulation. *Frontiers in Physics*, Volume 11 - 2023, 2023.
- [2] U.V. Catalyurek and C. Aykanat. Hypergraph-partitioning-based decomposition for parallel sparse-matrix vector multiplication. *IEEE Transactions on Parallel and Distributed Systems*, 10(7):673–693, 1999.
- [3] Gautam Gupta, Sivasankaran Rajamanickam, and Erik G. Boman. GAMGI: Communication-reducing algebraic multigrid for gpus. In *Proceedings of the 28th ACM SIGPLAN Annual Symposium on Principles and Practice of Parallel Programming (PPoPP)*, pages 61–75. ACM, 2024.
- [4] Cerebras Systems Inc. Wse-3 datasheet. <https://cerebras.net/product/system/>, 2024. DS03 v3 821.
- [5] George Karypis and Vipin Kumar. METIS: A Software Package for Partitioning Unstructured Graphs, Partitioning Meshes, and Computing Fill-Reducing Orderings of Sparse Matrices. Technical report, University of Minnesota, Department of Computer Science / Army HPC Research Center, 1997. Version 3.0.3.
- [6] Lawrence Livermore National Laboratory. Introduction to parallel computing tutorial. <http://hpc.llnl.gov/documentation/tutorials/introduction-parallel-computing-tutorial>, 2024. Accessed: 2025-05-08.
- [7] Nakul Manchanda and Karan Anand. Non-uniform memory access (numa). *New York University*, 4, 2010.

- [8] Duane Merrill and Michael Garland. Merge-based parallel sparse matrix-vector multiplication. In *SC '16: Proceedings of the International Conference for High Performance Computing, Networking, Storage and Analysis*, pages 678–689, 2016.
- [9] Peter Norvig. Latency numbers every programmer should know. <https://norvig.com/21-days.html#Latency>, 2021. Accessed: 2025-04-29.
- [10] Andreas Thune, Sven-Arne Reinemo, Tor Skeie, and Xing Cai. Detailed modeling of heterogeneous and contention-constrained point-to-point mpi communication. *IEEE Transactions on Parallel and Distributed Systems*, 34(5):1580–1593, 2023.
- [11] James D. Trotter, Sinan Ekmekçibaşı, Johannes Langguth, Tugba Torun, Emre Düzakin, Aleksandar Ilic, and Didem Unat. Bringing order to sparsity: A sparse matrix reordering study on multicore cpus. In *Proceedings of the International Conference for High Performance Computing, Networking, Storage and Analysis*, SC '23, New York, NY, USA, 2023. Association for Computing Machinery.
- [12] Cong Zheng, Shuo Gu, Tong-Xiang Gu, Bing Yang, and Xing-Ping Liu. Biell: A bisection ellpack-based storage format for optimizing spmv on gpus. *Journal of Parallel and Distributed Computing*, 74(7):2639–2647, 2014. Special Issue on Perspectives on Parallel and Distributed Processing.